2015

Stress-dependent second-order grain statistics of polycrystals

Christopher M. Kube
University of Nebraska-Lincoln, ckube@huskers.unl.edu

Joseph A. Turner
University of Nebraska-Lincoln, jaturner@unl.edu

Stress-dependent second-order grain statistics of polycrystals

Christopher M. Kube[a] and Joseph A. Turner
Department of Mechanical and Materials Engineering, University of Nebraska-Lincoln, W342 Nebraska Hall, Lincoln, Nebraska 68588-0526, USA

(Received 1 June 2015; revised 4 August 2015; accepted 16 September 2015; published online 30 October 2015)

In this article, the second-order statistics of the elastic moduli of randomly oriented grains in a polycrystal are derived for the case when an initial stress is present. The initial stress can be either residual stress or stresses generated from external loading. The initial stress is shown to increase or decrease the variability of the grain's elastic moduli from the average elastic moduli of the polycrystal. This variation in the elastic properties of the individual grains causes acoustic scattering phenomenon in polycrystalline materials to become stress-dependent. The influence of the initial stress on scattering is shown to be greater than the influence on acoustic phase velocities, which defines the acoustoelastic effect. This work helps the development of scattering based tools for the nondestructive analysis of material stresses in polycrystals. © *2015 Acoustical Society of America*.
[http://dx.doi.org/10.1121/1.4932026]

[MD] Pages: 2613–2625

I. INTRODUCTION

Ultrasonic grain scattering describes the interaction and scattering of ultrasonic waves from grain boundaries in polycrystalline materials. The scattering is a result of adjacent grains having relative differences in orientation. The orientation difference creates an impedance mismatch at the grain boundary between the adjacent grains. Because the scattering occurs at the grain boundaries, measurements of ultrasonic scattering are sensitive to microstructural features and changes. In previous studies, ultrasonic grain scattering has been employed to extract measurements of grain dimensions, grain shape, and elastic properties.[1–13] Turner and coworkers have developed robust measurement models that allow the average grain diameter of equiaxed grains to be determined with high precision.[1–4] Other researchers have applied similar models in order to estimate non-spherical grain dimensions and shapes.[5–10] Additional research has focused on using ultrasonic grain scattering measurements to estimate the elastic properties of polycrystalline materials.[11–13]

Additive manufactured materials is one area that could benefit from ultrasonic scattering based techniques. The increased use of additive manufacturing has led to the possibility of developing materials with tailored or customized microstructures. Customization could allow the materials engineer to optimize the material response and cater to its intended application. Then, ultrasonic scattering could be used to confirm the integrity of the manufactured part. Such measurements can be incorporated into a quality control setting in order to confirm the desired microstructural properties are in place during and after the additive manufacturing process. Residual stress is one property that is important to understand and possibly control in order to construct the desired part.[14–16] These internal stresses cause feature distortion and possible poor fusion or disbonding of layers.[14–16] These issues are especially prominent for manufactured parts with thin walls, parts with overhangs, and parts with tight geometrical tolerances.[14–16]

These present and future demands involving residual stress analysis has motivated the development of using ultrasonic grain scattering as a stress monitoring tool. The idea of relating stress to grain scattering was first proposed by Turner and Ghoshal[17] and was later explored experimentally by Kube *et al.*[18,19] However, the theory of Turner and Ghoshal was developed for materials under applied loads[17] rather than materials with residual stress. Residual stresses are formed from complex thermomechanical plastic deformation processes. Thus, modeling ultrasonic grain scattering from polycrystalline materials having residual stresses requires additional considerations.

In this article, the theoretical foundation relating ultrasonic grain scattering to residual stresses is derived. Effective stress-dependent stiffness tensors, $\mathbf{C}^{\text{eff}}$, which define the acoustoelastic effect for single crystals, are used as the orientation dependent stiffness of individual grains. The intensity of ultrasound scattered from an aggregate of stressed grains requires the eighth-rank stress-dependent covariance tensor $\boldsymbol{\Xi}$, which is a measure of the average spatial variation of the grain stiffnesses. A procedure for determining all components of $\boldsymbol{\Xi}$ is provided. The sensitivity of $\boldsymbol{\Xi}$ to stress magnitudes is compared with the ensemble average of $\mathbf{C}^{\text{eff}}$, which allows us to estimate the measurement resolution of a scattering based approach to traditional acoustoelastic phase velocity techniques for stress evaluation.

The article is organized as follows. Section II provides the background and derivation of the stress-dependent covariance tensor $\boldsymbol{\Xi}$. The resulting expressions provide all of the necessary elastic tensors needed to evaluate the stress-dependence of scattering based models such as ultrasonic attenuation[20–22] or diffuse ultrasonic grain scattering. The quantitative evaluation of $\boldsymbol{\Xi}$ is provided in Sec. III. These

[a]Electronic mail: ckube@huskers.unl.edu

results indicate that ultrasonic scattering based phenomenon in polycrystalline materials has a stress dependence greater than techniques based on classical acoustoelasticity. This work supports the potential for the development of accurate and sensitive ultrasonic based tools for the nondestructive evaluation of residual stresses.

II. THEORY

For polycrystalline media, scattering of ultrasonic waves from grain boundaries is intimately related to the scattering of ultrasound from internal inhomogeneities. As a bulk wave propagates in a direction through the polycrystal, each grain boundary along the propagation path has a potential to scatter a portion of the wave's energy into various directions. The resultant scattering is caused by the deviation of elastic properties between the volume of grains contributing to the scattering process and the mean elastic properties of the polycrystal, $\delta\mathbf{C}(\mathbf{x}) = \mathbf{C}(\mathbf{x}) - \mathbf{C}^0$. In this case, $\mathbf{C}(\mathbf{x})$ is the elastic modulus tensor of a grain located at the spatial position $\mathbf{x}$ while $\mathbf{C}^0$ is the macroscopic elastic stiffness of the polycrystal. Thus, each grain can act as an inhomogeneity while, in a statistical sense, all of the other grains constitute a homogeneous medium surrounding the inhomogeneous grain. This concept motivates the use of perturbation theory to model wave propagation and grain scattering in random elastic media.[20–25] In such theories, the second- and higher-order perturbations are able to capture the losses of energy from the mean or average wave field due to scattering at grain boundaries.

Second-order perturbations to the mean wave field depend on the statistical covariance of the stochastic tensors $\delta\mathbf{C}(\mathbf{x})$ and $\delta\mathbf{C}(\mathbf{x}')$, where $\mathbf{x}'$ is another position vector to a different point in the polycrystal. The covariance is then defined as

$$\boldsymbol{\xi}(\mathbf{x},\mathbf{x}') = \langle \delta\mathbf{C}(\mathbf{x})\delta\mathbf{C}(\mathbf{x}')\rangle - \langle \delta\mathbf{C}(\mathbf{x})\rangle\langle \delta\mathbf{C}(\mathbf{x}')\rangle, \tag{1}$$

where the operation $\langle\cdots\rangle$ defines the expectation or average value. For tensors defining physical properties of polycrystals, the average value of the tensor is achieved using orientation averages over all possible rotational transformations. Details of ensemble and orientation averaging of tensors can be located in Kröner's treatise.[26]

Carrying out the orientation average in Eq. (1) requires, first, the decoupling of the spatial and tensorial components, which is achieved by assuming the grain orientations are uncorrelated spatially.[26,27] With this assumption, Eq. (1) is given as

$$\xi_{ijkl}^{\alpha\beta\gamma\delta}(\mathbf{x},\mathbf{x}') = [\langle \delta C_{ijkl}\delta C_{\alpha\beta\gamma\delta}\rangle - \langle \delta C_{ijkl}\rangle\langle \delta C_{\alpha\beta\gamma\delta}\rangle]\eta(\mathbf{x}-\mathbf{x}'), \tag{2}$$

where $\eta(\mathbf{x}-\mathbf{x}')$ is a two-point correlation function of the random and macroscopically homogeneous medium.[28] The spatial dependency $\mathbf{x}-\mathbf{x}'$ reduces to the magnitude $|\mathbf{x}-\mathbf{x}'|$ if the polycrystal is statistically isotropic. The spatially-independent, tensorial part of the covariance is

$$\Xi_{ijkl}^{\alpha\beta\gamma\delta} = \langle \delta C_{ijkl}\delta C_{\alpha\beta\gamma\delta}\rangle - \langle \delta C_{ijkl}\rangle\langle \delta C_{\alpha\beta\gamma\delta}\rangle, \tag{3}$$

whose average is obtained using the method first proposed by Morris.[29]

The tensor $\boldsymbol{\Xi}$ is a statistical covariance measure between different components of the fourth-rank elastic moduli. $\boldsymbol{\Xi}$ reduces to a measure of statistical variance when the components of the elastic moduli are equal, i.e., $i=\alpha$, $j=\beta$, $k=\gamma$, $l=\delta$. Physically, the variance of the elastic moduli gives an average measure of the difference between the stiffness of a single grain to the stiffness of the polycrystal ensemble. Thus, the intensity of ultrasound scattered from grain boundaries directly scales with the magnitude of $\boldsymbol{\Xi}$. The magnitude of $\boldsymbol{\Xi}$ depends strongly on the degree of the elastic anisotropy of individual grains along with the macroscopic elastic anisotropy of the bulk polycrystal. For example, if the polycrystal contains grains of cubic elastic symmetry and has macroscopic elastic properties of orthorhombic symmetry, the magnitude of $\boldsymbol{\Xi}$ is a function of the elastic anisotropy constant for single-crystals $\nu = c_{11} - c_{12} - 2c_{44}$ along with the 12 macroscopic elastic anisotropy constants W_{400}, W_{420}, W_{440}, W_{600}, W_{620}, W_{640}, W_{660}, W_{800}, W_{820}, W_{840}, W_{860}, and W_{880}.[30]

In this article, the variation of the grain-to-grain elastic properties caused by a homogeneous material stress is considered. This variation is naturally captured using the covariance tensor $\boldsymbol{\Xi}$. The material stress influences $\boldsymbol{\Xi}$ in two distinct ways. First, if the stress is not hydrostatic, the polycrystal will exhibit a stress-induced anisotropy of the polycrystals macroscopic elastic properties. In this case, the elastic moduli of the individual grains gain symmetry dependence about the principle directions of the material stress. Second, the stress (including hydrostatic) causes the elastic properties of the individual grains to differ further from the average elastic properties of the polycrystal.

The characterization of the stress-dependence in $\boldsymbol{\Xi}$ was first given by Turner and Ghoshal[17] and later demonstrated experimentally by Kube *et al.*[18,19] The present theory utilizes a more commonly used elastic constitutive relation,[31–37] which is valid for both residual and mechanical stresses. This constitutive relation leads to different stress-dependent elastic properties than those given by Turner and Ghoshal.[17] An error involving the compliance relation to the shear constant c_{44} used in the calculations of Turner and Ghoshal is also corrected here [see Eq. (A5) in Appendix A].[17]

The theory is divided into two sections, which result in the outcome of an expression for the stress-dependent eighth-rank covariance tensor $\boldsymbol{\Xi}$. Section II A follows from the theory of acoustoelasticity developed by Man and coworkers and Huang *et al.*[31–37] In this treatment, a constitutive relation for elastic media containing an initial stress is employed in order to derive equations of motion for a small-amplitude harmonic plane wave. A stress-dependent Christoffel equation follows from the equation of motion, which is applicable to materials belonging to any crystallographic symmetry group. From this Christoffel equation, definitions of the stress-dependent effective elastic moduli $\mathbf{C}^{\text{eff}}$ are obtained. The orientation dependent parts of $\mathbf{C}^{\text{eff}}$

allow its components to be written with respect to a general coordinate system. This description allows $\mathbf{C}^{\text{eff}}$ to represent the stiffness of an individual crystallite or grain having a specific orientation. A method of polycrystalline homogenization is used in Sec. II B to define the stress-dependent effective elastic moduli of the polycrystal by making use of ensemble averages on $\mathbf{C}^{\text{eff}}$. Finally, Sec. II C defines the covariance tensor in the form $\Xi_{ijkl}^{\alpha\beta\gamma\delta} = \langle C_{ijkl}^{\text{eff}} C_{\alpha\beta\gamma\delta}^{\text{eff}} \rangle - \langle C_{ijkl}^{\text{eff}} \rangle \langle C_{\alpha\beta\gamma\delta}^{\text{eff}} \rangle$, which is a function of the initial stress $\boldsymbol{\sigma}$.

A. Stress-dependent Christoffel equation for a single grain or crystallite

An appropriate constitutive relation is needed in order to represent the situation of elastic wave propagation in a material containing an initial stress. Constitutive relations based on hyperelastic material models provided the first attempts to address acoustoelasticity.[38–40] These early models considered the initial stress to be a result of a deformation process that takes the material from a natural material configuration to an initial configuration. Then, an infinitesimal displacement of a small-amplitude elastic wave is superimposed on the initial deformation in order to bring the material into its current configuration. However, Pao *et al*. pointed out that residual stresses are often manifest due to inhomogeneous processes involving plastic deformation, which are not able to be properly represented with a hyperelastic material model.[41] Observing the need for an improved model, Man and Lu proposed a constitutive relation based on linear elasticity and the incremental elasticity tensor.[31] A constitutive relation of this form is able to represent a material in its initially stressed configuration. Thus, the possible complex plastic deformation processes that led to the initial state of stress are of no concern. A number of models for acoustoelasticity[32–37] related closely to the formalism of Man and Lu[31] followed. Due to the advantage of its applicability to materials having residual stresses, we adopt their form of the constitutive relation valid for polycrystalline materials with an initial stress[33,37]

$$P_{ij} = \sigma_{ij} + C_{ijkl}E_{kl} + (-C_{ijkl}S_{rrmn} + C_{ijkr}S_{rlmn} + C_{ijrl}S_{rkmn} + C_{irkl}S_{rjmn} + C_{rjkl}S_{rimn} + C_{ijklrs}S_{rsmn})\sigma_{mn}E_{kl}, \quad (4)$$

where $\mathbf{P}$ is the second Piola-Kirchoff stress tensor, and $\boldsymbol{\sigma}$ is the initial (Cauchy) stress tensor. C_{ijkl} and S_{ijkl} define the second-order elastic modulus and compliance tensors, respectively. They are related through the identity tensor $C_{ijmn}S_{mnkl} = I_{ijkl} = (\delta_{ik}\delta_{jl} + \delta_{il}\delta_{jk})/2$. C_{ijklmn} is a sixth-rank tensor that defines the third-order elastic constants. In this article, Eq. (4) is used to define the constitutive relation for a single grain contained in the polycrystal. Each grain in the polycrystal is assumed to contain the same crystallographic symmetries as a single-crystal. Thus, C_{ijkl}, C_{ijklmn}, and S_{ijkl} are defined using the point group symmetries of single crystals. The governing equation of motion for the wave displacement, which includes the initial stress $\boldsymbol{\sigma}$, is

$$P_{ij,j} = \rho u_{i,tt}, \quad (5)$$

where ρ is the density of the grain and $_{,i}$ implies the partial spatial derivative. Assuming the displacement is a time-harmonic plane wave, the equation of motion can be reduced to the stress-dependent Christoffel equations,

$$[\Lambda_{ijkl}\hat{n}_j\hat{n}_l + (\sigma_{jl}\hat{n}_j\hat{n}_l - \rho V^2)\delta_{ik}]u_i = 0. \quad (6)$$

The tensor $\boldsymbol{\Lambda}$ is of fourth-rank and depends on the elastic constants of the grain and the initial stress,

$$\Lambda_{ijkl} = C_{ijkl} + (-C_{ijkl}S_{rrpq} + C_{ijkr}S_{rlpq} + C_{ijrl}S_{rkpq} + C_{irkl}S_{rjpq} + C_{rjkl}S_{ripq} + C_{ijklmn}S_{mnpq})\sigma_{pq}. \quad (7)$$

Equation (7) is the analog to the "load-dependent effective elastic moduli G_{ijkl}" defined in Eq. (1) of Turner and Ghoshal.[17] These two definitions are not equivalent; the expression in Eq. (1) of Turner and Ghoshal[17] is derived using a different constitutive relation. Additionally, $\boldsymbol{\Lambda}$ is only part of the effective stress-dependent elastic moduli, which will be defined in Eq. (9). The three eigenvalue solutions to Eq. (6) represent the phase velocities (V) of one quasi-longitudinal, one transverse, and one quasi-transverse wave. The propagation direction is given by $\hat{\mathbf{n}}$ while the three displacement directions are obtained from the eigenvectors u_i. The traditional Christoffel equation for wave propagation in unstressed crystals is

$$[C_{ijkl}\hat{n}_j\hat{n}_l - \rho V^2\delta_{ik}]u_i = 0. \quad (8)$$

By comparing Eqs. (6) and (8), we define the effective stress-dependent elastic modulus tensor as

$$C_{ijkl}^{\text{eff}} = \Lambda_{ijkl} + \delta_{ik}\sigma_{jl} = C_{ijkl} + (-C_{ijkl}S_{rrpq} + C_{ijkr}S_{rlpq} + C_{ijrl}S_{rkpq} + C_{irkl}S_{rjpq} + C_{rjkl}S_{ripq} + C_{ijklmn}S_{mnpq})\sigma_{pq} + \delta_{ik}\sigma_{jl}. \quad (9)$$

The definition of $\mathbf{C}^{\text{eff}}$ in Eq. (9) is valid for crystals belonging to any of the crystallographic symmetry classes assuming the tensors representing the second- and third-order elastic constants are available. A procedure to construct these tensors is given in Appendix A. It is important to note that a state of stress results in the crystallite having *effective* elastic properties while the single-crystal elastic constants given in C_{ijkl}, C_{ijklmn}, and S_{ijkl} are assumed to be physical material parameters unchanged by the stress. Furthermore, the tensor defining the initial stress $\boldsymbol{\sigma}$ is appropriate for either residual or mechanical stresses. In Sec. II B, $\mathbf{C}^{\text{eff}}$ is homogenized in order to define the stress-dependent effective elastic properties of the polycrystal.

B. Homogenization of $\mathbf{C}^{\text{eff}}$

In Sec. II A, the definition of $\mathbf{C}^{\text{eff}}$ represents the effective stress-dependent elastic modulus tensor of a particular grain in the polycrystal. The tensors of single-crystal elastic moduli C_{ijkl}, C_{ijklmn}, and compliance S_{ijkl}, found within the definition of $\mathbf{C}^{\text{eff}}$, depend on the orientation Ω of the grain. The definitions of C_{ijkl}, C_{ijklmn}, and S_{ijkl} for cubic crystallite

symmetry are found in Appendix A where they are written in an invariant form as functions of orientation dependent rotation matrices $[\mathbf{a}(\Omega)]$. The continuous distribution of grains and their random orientations allows the elastic properties of the individual grains to be treated as stochastic variables. Thus, statistical measures on these variables are used to estimate the macroscopic elastic properties of the bulk polycrystal. This process of merging the properties of the heterogeneous microscale with the homogeneous macroscale of the polycrystal is referred to as statistical homogenization. Voigt was the first to propose that the average elastic moduli over all possible orientation of a single crystallite could be used to give the elastic moduli of the macroscopically homogeneous polycrystal.[42] A large number of more advanced techniques have been developed over the decades, which are outside the scope of this article. Readers should consult the works of Kröner,[26,27] Watt *et al.*,[43] and Hirsekorn[44] for overviews on the topic.

The present article is concerned with the statistical quantities related to the stress-dependent elastic properties of the polycrystal. Using the definition of $\mathbf{C}^{\text{eff}}$, a Voigt-type average over all possible orientations of $\mathbf{C}^{\text{eff}}$ is given by

$$\langle C^{\text{eff}}_{ijkl}(\Omega)\rangle = \int_{\Omega} w(\Omega)\, C^{\text{eff}}_{ijkl}(\Omega)\mathrm{d}\Omega, \tag{10}$$

where Ω defines the space of possible orientations and $w(\Omega)$ is a probability distribution function that defines the grain orientation probability. $w(\Omega) = 1$ for the case for which all orientations of the grains are equally likely. $\langle \mathbf{C}^{\text{eff}}(\Omega)\rangle$ is defined as the effective stress-dependent elastic moduli of the polycrystal. Equation (10) explicitly indicates the dependence of $\mathbf{C}^{\text{eff}}$ on the orientation Ω of the grain. The orientation dependence is introduced in the definitions of C_{ijkl}, C_{ijklmn}, and S_{ijkl} through the rotation matrices $[\mathbf{a}(\Omega)]$ in Eq. (A1) of Appendix A. The orientation dependence of $\mathbf{C}^{\text{eff}}_{ijkl}$ will be implicitly assumed in the remainder of the article. Substitution of Eq. (9) into Eq. (10) gives

$$\begin{aligned}\langle C^{\text{eff}}_{ijkl}\rangle &= \langle \Lambda_{ijkl}\rangle + \delta_{ik}\sigma^0_{jl}\\ &= \langle C_{ijkl}\rangle + (-\langle C_{ijkl}S_{rrpq}\rangle + \langle C_{ijkr}S_{rlpq}\rangle\\ &\quad + \langle C_{ijrl}S_{rkpq}\rangle + \langle C_{irkl}S_{rjpq}\rangle + \langle C_{rjkl}S_{ripq}\rangle\\ &\quad + \langle C_{ijklmn}S_{mnpq}\rangle)\sigma^0_{pq} + \delta_{ik}\sigma^0_{jl},\end{aligned} \tag{11}$$

where we have assumed that the homogeneous initial stress present in the polycrystal is equal to the average stress present in all of the grains, i.e., $\sigma^0_{ij} = \langle \sigma_{ij}\rangle$. Equation (11) could be used to solve for the stress-dependent phase velocities and wave displacements in a stressed polycrystal,

$$[\langle C^{\text{eff}}_{ijkl}\rangle \hat{n}_j\hat{n}_l - \rho V^2\delta_{ik}]u_i = 0. \tag{12}$$

Equation (12) governs the propagation of bulk waves in stressed polycrystalline materials with material texture and grains belonging to any crystallographic symmetry class. Section II B 1 considers a limiting case of $\langle \mathbf{C}^{\text{eff}}\rangle$, in which the polycrystal is assumed to have grains of cubic crystallographic symmetry and is statistically isotropic when the material is free of stress.

1. $\langle \mathbf{C}^{\text{eff}}\rangle$ for polycrystals containing grains of cubic crystallographic symmetry

Equation (11) defines the effective stress-dependent elastic modulus tensor for polycrystalline materials. In this section, $\langle \mathbf{C}^{\text{eff}}\rangle$ is evaluated analytically for polycrystals that have statistically isotropic material symmetry and contain grains of cubic crystallographic symmetry. The definitions of C_{ijkl}, C_{ijklmn}, and S_{ijkl} are given by Eqs. (A3), (A4), and (A6) of Appendix A, respectively. It is convenient to separate the parts of C^{eff}_{ijkl} that are orientation dependent from the isotropic parts

$$C^{\text{eff}}_{ijkl} = C^I_{ijkl} + C^A_{ijkl} + (\bar{C}^I_{ijklpq} + \bar{C}^A_{ijklpq})\sigma_{pq} + \delta_{ik}\sigma_{jl}, \tag{13}$$

where the isotropic parts are

$$\begin{aligned}C^I_{ijkl} &= c_{12}\delta_{ij}\delta_{kl} + 2c_{44}I_{ijkl}, \text{ and}\\ \bar{C}^I_{ijklmn} &= [(c_{123} - c_{12})\nu_s + s_{12}(3c_{123} + 4c_{144} + 2d_2)\\ &\quad - c_{12}(2s_{44} - s_{12}) + 2c_{123}s_{44}]\delta_{ij}\delta_{kl}\delta_{mn}\\ &\quad + 2[\nu_s(c_{144} - c_{44}) + s_{12}(3c_{144} + 4c_{456} + 2d_3)\\ &\quad - c_{44}(2s_{44} - s_{12}) + 2c_{144}s_{44}]\delta_{mn}I_{ijkl}\\ &\quad + 4s_{44}[(c_{12} + c_{144})(\delta_{ij}I_{klmn} + \delta_{kl}I_{ijmn})\\ &\quad + (c_{44} + c_{456})(\delta_{ik}I_{jlmn} + \delta_{il}I_{jkmn})\\ &\quad + c_{456}(\delta_{im}I_{jnkl} + \delta_{in}I_{jmkl})\\ &\quad + c_{44}(\delta_{jl}I_{ikmn} + \delta_{jk}I_{ilmn})],\end{aligned} \tag{14}$$

while the orientation dependent parts are

$$\begin{aligned}C^A_{ijkl} &= \nu A_{ijkl}, \text{ and}\\ \bar{C}^A_{ijklmn} &= [2s_{44}d_1 + 4\nu\nu_s + \nu_s(d_1 + 8d_3)]A^1_{ijklmn}\\ &\quad + [2c_{12}\nu_s + 2s_{44}d_2 + \nu_s(2c_{144} + d_2)]A^2_{ijklmn}\\ &\quad + s_{44}(2d_3 + \nu)A^3_{ijklmn} - [2\nu_s(c_{12} + c_{144})\\ &\quad + \nu(s_{11} + 2s_{12}) - s_{12}(d_1 + 3d_2 + 8d_3)]\delta_{mn}A_{ijkl}\\ &\quad + [\nu_s(2c_{456} + d_3 + 2c_{44}) - \nu](\delta_{ik}A_{mjnl}\\ &\quad + \delta_{il}A_{mjkn} + \delta_{jk}A_{imnl} + \delta_{jl}A_{imkn}).\end{aligned} \tag{15}$$

The constants ν, ν_s, d_1, d_2, d_3 are functions of single-crystal elastic constants and are defined in Appendix A. The tensors A_{ijkl}, A^1_{ijklmn}, A^2_{ijklmn}, and A^3_{ijklmn} contain products of rotation matrices, which are also defined in Appendix A. $\langle \mathbf{C}^{\text{eff}}\rangle$ is obtained by finding the orientation averages of the orientation dependent parts of $\mathbf{C}^{\text{eff}}$,

$$\langle C^{\text{eff}}_{ijkl}\rangle = C^I_{ijkl} + \langle C^A_{ijkl}\rangle + (\bar{C}^I_{ijklpq} + \langle \bar{C}^A_{ijklpq}\rangle)\sigma^0_{pq} + \delta_{ik}\sigma^0_{jl}. \tag{16}$$

The computational burden in carrying out the averages is removed by using the definitions

$$\langle A_{ijkl}\rangle = \langle a_{iu}a_{ju}a_{ku}a_{lu}\rangle = \frac{1}{5}\left(\delta_{ij}\delta_{kl}+\delta_{ik}\delta_{jl}+\delta_{il}\delta_{jk}\right),$$
$$\begin{aligned}\langle A^1_{ijklmn}\rangle &= \langle a_{iu}a_{ju}a_{ku}a_{lu}a_{mu}a_{nu}\rangle \\ &= \frac{1}{7}\left(\delta_{ij}\langle A_{klmn}\rangle + \delta_{ik}\langle A_{jlmn}\rangle + \delta_{il}\langle A_{jkmn}\rangle\right. \\ &\quad \left. + \delta_{im}\langle A_{jkln}\rangle + \delta_{in}\langle A_{jklm}\rangle\right),\end{aligned} \tag{17}$$

which arrive from the tensor averaging procedure outlined in Appendix B.

Now, consider a case of uniaxial stress for which the only nonzero component of $\boldsymbol{\sigma}$ is σ_{33}. From Eq. (11), the tensor $\langle\boldsymbol{\Lambda}\rangle$ is needed to define $\langle\mathbf{C}^{\text{eff}}\rangle$. Let $\boldsymbol{\Lambda}^0 = \langle\boldsymbol{\Lambda}\rangle$ denote the orientation average of $\boldsymbol{\Lambda}$. Because of the uniaxial stress, the tensorial form of $\boldsymbol{\Lambda}^0$ exhibits transversely isotropic symmetry about the symmetry axis in the direction of the stress. It is important to note that $\boldsymbol{\Lambda}^0$ is a statistically defined tensor representing the macroscopic elastic properties. Thus, macroscopically, the polycrystal exhibits a stress-induced anisotropy. However, the symmetry of the elastic tensors C_{ijkl}, C_{ijklmn}, and S_{ijkl} remain unchanged when a stress is present. $\boldsymbol{\Lambda}^0$ can be defined using five independent components where the non-zero components are: $\Lambda^0_{11} = \Lambda^0_{22}$, Λ^0_{12}, $\Lambda^0_{13} = \Lambda^0_{23}$, Λ^0_{33}, $\Lambda^0_{44} = \Lambda^0_{55}$, $\Lambda^0_{66} = (\Lambda^0_{11} - \Lambda^0_{12})/2$, and $\Lambda^0_{IJ} = \Lambda^0_{JI}$. Using the definitions in Eq. (17), the five independent components of $\boldsymbol{\Lambda}^0$ are given as

$$\begin{aligned}
\Lambda^0_{11} &= c_{12} + 2c_{44} + \frac{3\nu}{5} + \frac{1}{35}(35c_{123}\nu_s - 14c_{44}\nu_s - 7c_{12}\nu_s + 98c_{144}\nu_s + 56c_{456}\nu_s + 21s_{12}d_1 \\
&\quad + 133s_{12}d_2 + 308s_{12}d_3 + 6s_{44}d_1 + 70s_{44}d_2 + 56s_{44}d_3 + 21s_{12}\nu - 42s_{44}\nu + 3d_1\nu_s \\
&\quad + 35d_2\nu_s + 52d_3\nu_s - 9\nu\nu_s + 35c_{12}s_{12} - 70c_{12}s_{44} + 70c_{44}s_{12} - 140c_{44}s_{44} + 105c_{123}s_{12} \\
&\quad + 350c_{144}s_{12} + 70c_{123}s_{44} + 140c_{144}s_{44} + 280c_{456}s_{12})\sigma_{33}, \\
\Lambda^0_{12} &= c_{12} + \frac{\nu}{5} + \frac{1}{35}(35c_{123}\nu_s - 7c_{12}\nu_s + 28c_{144}\nu_s + 7s_{12}d_1 + 91s_{12}d_2 + 56s_{12}d_3 + 2s_{44}d_1 \\
&\quad + 42s_{44}d_2 + 7s_{12}\nu - 14s_{44}\nu + d_1\nu_s + 21d_2\nu_s + 8d_3\nu_s - 3\nu\nu_s + 35c_{12}s_{12} - 70c_{12}s_{44} \\
&\quad + 105c_{123}s_{12} + 140c_{144}s_{12} + 70c_{123}s_{44})\sigma_{33}, \\
\Lambda^0_{13} &= c_{12} + \frac{\nu}{5} + \frac{1}{35}(21c_{12}\nu_s + 35c_{123}\nu_s + 56c_{144}\nu_s + 7s_{12}d_1 + 91s_{12}d_2 + 56s_{12}d_3 + 6s_{44}d_1 \\
&\quad + 70s_{44}d_2 + 56s_{44}d_3 + 7s_{12}\nu + 14s_{44}\nu + 3d_1\nu_s + 35d_2\nu_s + 24d_3\nu_s + 5\nu\nu_s + 35c_{12}s_{12} \\
&\quad + 70c_{12}s_{44} + 105c_{123}s_{12} + 140c_{144}s_{12} + 70c_{123}s_{44} + 140c_{144}s_{44})\sigma_{33}, \\
\Lambda^0_{33} &= c_{12} + 2c_{44} + \frac{3\nu}{5} + \frac{1}{35}(49c_{12}\nu_s + 98c_{44}\nu_s + 35c_{123}\nu_s + 154c_{144}\nu_s + 168c_{456}\nu_s + 21s_{12}d_1 \\
&\quad + 133s_{12}d_2 + 308s_{12}d_3 + 30s_{44}d_1 + 126s_{44}d_2 + 504s_{44}d_3 + 21s_{12}\nu + 126s_{44}\nu + 15d_1\nu_s \\
&\quad + 63d_2\nu_s + 204d_3\nu_s + 39\nu\nu_s + 35c_{12}s_{12} + 210c_{12}s_{44} + 70c_{44}s_{12} + 420c_{44}s_{44} \\
&\quad + 105c_{123}s_{12} + 350c_{144}s_{12} + 70c_{123}s_{44} + 420c_{144}s_{44} + 280c_{456}s_{12} + 560c_{456}s_{44})\sigma_{33}, \\
\Lambda^0_{44} &= c_{44} + \frac{\nu}{5} + \frac{1}{35}(21c_{44}\nu_s + 35c_{144}\nu_s + 56c_{456}\nu_s + 7s_{12}d_1 + 21s_{12}d_2 + 126s_{12}d_3 + 6s_{44}d_1 \\
&\quad + 14s_{44}d_2 + 112s_{44}d_3 + 7s_{12}\nu + 14s_{44}\nu + 3d_1\nu_s + 7d_2\nu_s + 52d_3\nu_s + 5\nu\nu_s + 35c_{44}s_{12} \\
&\quad + 70c_{44}s_{44} + 105c_{144}s_{12} + 70c_{144}s_{44} + 140c_{456}s_{12} + 140c_{456}s_{44})\sigma_{33}.
\end{aligned} \tag{18}$$

Finally, using Eq. (18), $\langle\mathbf{C}^{\text{eff}}\rangle$ is written in a general form

$$\begin{aligned}\langle C^{\text{eff}}_{ijkl}\rangle &= \Lambda^0_{12}\delta_{ij}\delta_{kl} + \left(\Lambda^0_{11} - \Lambda^0_{12}\right)I_{ijkl} + \left(\Lambda^0_{13} - \Lambda^0_{12}\right)\left(\delta_{ij}\hat{e}_k\hat{e}_l + \delta_{kl}\hat{e}_i\hat{e}_j\right) - \frac{1}{2}\left(\Lambda^0_{11} - \Lambda^0_{12} - 2\Lambda^0_{44}\right) \\ &\quad \times \left(\delta_{ik}\hat{e}_j\hat{e}_l + \delta_{il}\hat{e}_j\hat{e}_k + \delta_{jk}\hat{e}_i\hat{e}_l + \delta_{jl}\hat{e}_i\hat{e}_k\right) + \left(\Lambda^0_{11} + \Lambda^0_{33} - 2\Lambda^0_{13} - 4\Lambda^0_{44}\right)\hat{e}_i\hat{e}_j\hat{e}_k\hat{e}_l + \delta_{ik}\sigma^0_{jl},\end{aligned} \tag{19}$$

where the unit vector $\hat{\mathbf{e}}$ is in the direction of the uniaxial stress.

C. Stress-dependent covariance tensor, Ξ

The stress-independent covariance tensor was defined in Eq. (3). In order to construct the stress-dependent covariance tensor, the deviation of the effective stress-dependent moduli from the mean elastic moduli of the polycrystal is given as

$$\delta C^{\text{eff}}_{ijkl} = C^{\text{eff}}_{ijkl} - \langle C^{\text{eff}}_{ijkl}\rangle. \tag{20}$$

For polycrystals with randomly oriented grains, $\langle\delta\mathbf{C}^{\text{eff}}\rangle = 0$. Using Eq. (20), the stress-dependent covariance is

$$\Xi_{ijkl}^{\alpha\beta\gamma\delta} = \langle \delta C_{ijkl}^{\text{eff}} \delta C_{\alpha\beta\gamma\delta}^{\text{eff}} \rangle - \langle \delta C_{ijkl}^{\text{eff}} \rangle \langle \delta C_{\alpha\beta\gamma\delta}^{\text{eff}} \rangle$$
$$= \langle C_{ijkl}^{\text{eff}} C_{\alpha\beta\gamma\delta}^{\text{eff}} \rangle - \langle C_{ijkl}^{\text{eff}} \rangle \langle C_{\alpha\beta\gamma\delta}^{\text{eff}} \rangle. \quad (21)$$

Now, if the initial stress is uniaxial with σ_{33} as the only non-zero component, Eq. (21) simplifies to the form

$$\Xi_{ijkl}^{\alpha\beta\gamma\delta} = \langle C_{ijkl}^{A} C_{\alpha\beta\gamma\delta}^{A} \rangle - \langle C_{ijkl}^{A} \rangle \langle C_{\alpha\beta\gamma\delta}^{A} \rangle$$
$$+ (\langle C_{\alpha\beta\gamma\delta}^{A} \bar{C}_{ijkl33}^{A} \rangle - \langle C_{\alpha\beta\gamma\delta}^{A} \rangle \langle \bar{C}_{ijkl33}^{A} \rangle$$
$$+ \langle C_{ijkl}^{A} \bar{C}_{\alpha\beta\gamma\delta33}^{A} \rangle - \langle C_{ijkl}^{A} \rangle \langle \bar{C}_{\alpha\beta\gamma\delta33}^{A} \rangle) \sigma_{33}$$
$$+ (\langle \bar{C}_{ijkl33}^{A} \bar{C}_{\alpha\beta\gamma\delta33}^{A} \rangle - \langle \bar{C}_{ijkl33}^{A} \rangle \langle \bar{C}_{\alpha\beta\gamma\delta33}^{A} \rangle) \sigma_{33}^{2}. \quad (22)$$

The orientation averages needed to evaluate the components of $\boldsymbol{\Xi}$ can be found in Appendix B. Unlike in Turner and Ghoshal,[17] the averaging procedure in Appendix B allows analytic expressions of the components of $\boldsymbol{\Xi}$ to be given in closed-form in terms of second- and third-order single-crystal elastic constants. Out of the possible 6561 components of the eighth-rank $\boldsymbol{\Xi}$, only 44 of them are independent when considering a uniaxial stress (σ_{33}), i.e., $\boldsymbol{\Xi}$ has transversely isotropic symmetry. The 44 independent components are Ξ_{1111}^{1111}, Ξ_{1111}^{1122}, Ξ_{1111}^{1133}, Ξ_{1111}^{1212}, Ξ_{1111}^{1313}, Ξ_{1111}^{2222}, Ξ_{1111}^{2233}, Ξ_{1111}^{2323}, Ξ_{1111}^{3333}, Ξ_{1112}^{1112}, Ξ_{1112}^{1222}, Ξ_{1112}^{1233}, Ξ_{1112}^{1323}, Ξ_{1113}^{1113}, Ξ_{1113}^{1223}, Ξ_{1113}^{1322}, Ξ_{1113}^{1333}, Ξ_{1122}^{1122}, Ξ_{1122}^{1133}, Ξ_{1122}^{1212}, Ξ_{1122}^{1313}, Ξ_{1122}^{3333}, Ξ_{1123}^{1123}, Ξ_{1123}^{1213}, Ξ_{1123}^{2333}, Ξ_{1133}^{1133}, Ξ_{1133}^{1212}, Ξ_{1133}^{1313}, Ξ_{1133}^{2233}, Ξ_{1133}^{2323}, Ξ_{1133}^{3333}, Ξ_{1212}^{1212}, Ξ_{1212}^{1313}, Ξ_{1212}^{3333}, Ξ_{1213}^{1213}, Ξ_{1213}^{2333}, Ξ_{1233}^{1233}, Ξ_{1233}^{1323}, Ξ_{1313}^{1313}, Ξ_{1313}^{2323}, Ξ_{1313}^{3333}, Ξ_{1323}^{1323}, Ξ_{1333}^{1333}, and Ξ_{3333}^{3333}. Relations between the 44 independent components of $\boldsymbol{\Xi}$ and the remaining 1597 non-zero terms are listed elsewhere.[45] Section III gives quantitative results for these 44 components for polycrystalline iron and aluminum.

III. RESULTS AND DISCUSSION

The quantitative evaluation of $\langle \mathbf{C}^{\text{eff}} \rangle$ and $\boldsymbol{\Xi}$ allows their importance to be highlighted. In this section, the analysis is restricted to macroscopically isotropic polycrystals with grains of cubic crystallographic symmetry and a uniaxial stress σ_{33}, which allows the use of the definitions given in Sec. I. Each component of $\langle \mathbf{C}^{\text{eff}} \rangle$ and $\boldsymbol{\Xi}$ can be written in terms of coefficients that signify the relative dependence to the uniaxial stress. A linear form of $\langle \mathbf{C}^{\text{eff}} \rangle$ is given by

$$\langle C_{ijkl}^{\text{eff}} \rangle = L_0 + L_1 \sigma_{33}, \quad (23)$$

where $L_0 = \langle C_{ijkl} \rangle$ and $L_1 = \bar{C}_{ijklpq}^{I} + \langle \bar{C}_{ijklpq}^{A} \rangle + \delta_{ik}$. The stress-dependent covariance can be written in a quadratic form

$$\Xi_{ijkl}^{\alpha\beta\gamma\delta} = K_0 + K_1 \sigma_{33} + K_2 \sigma_{33}^2, \quad (24)$$

where K_0, K_1, and K_2 are given by

TABLE I. Single-crystal elastic constants for iron (Refs. 21 and 46) and aluminum (Ref. 46) (GPa).

	c_{11}	c_{12}	c_{44}	c_{111}	c_{112}	c_{123}	c_{144}	c_{166}	c_{456}
Fe	219.2	136.8	109.2	−2720	−608	−578	−836	−530	−720
Al	107	61	28	−1080	−315	36	−23	−340	−30

TABLE II. Stress-dependent elastic moduli for iron defined in terms of the coefficients L_0 (GPa) and L_1 (dimensionless).

	$\langle C_{11}^{\text{eff}} \rangle$	$\langle C_{12}^{\text{eff}} \rangle$	$\langle C_{13}^{\text{eff}} \rangle$	$\langle C_{33}^{\text{eff}} \rangle$	$\langle C_{44}^{\text{eff}} \rangle$	$\langle C_{66}^{\text{eff}} \rangle$
L_0	273.6	109.6	109.6	273.6	82.0	82.0
L_1	−0.406	0.8666	−1.8075	−7.6910	−0.2788	−0.4536

$$K_0 = \langle C_{ijkl}^{A} C_{\alpha\beta\gamma\delta}^{A} \rangle - \langle C_{ijkl}^{A} \rangle \langle C_{\alpha\beta\gamma\delta}^{A} \rangle,$$
$$K_1 = \langle C_{\alpha\beta\gamma\delta}^{A} \bar{C}_{ijkl33}^{A} \rangle - \langle C_{\alpha\beta\gamma\delta}^{A} \rangle \langle \bar{C}_{ijkl33}^{A} \rangle + \langle C_{ijkl}^{A} \bar{C}_{\alpha\beta\gamma\delta33}^{A} \rangle$$
$$- \langle C_{ijkl}^{A} \rangle \langle \bar{C}_{\alpha\beta\gamma\delta33}^{A} \rangle,$$
$$K_2 = \langle \bar{C}_{ijkl33}^{A} \bar{C}_{\alpha\beta\gamma\delta33}^{A} \rangle - \langle \bar{C}_{ijkl33}^{A} \rangle \langle \bar{C}_{\alpha\beta\gamma\delta33}^{A} \rangle. \quad (25)$$

The coefficients L_0, L_1, K_0, K_1, and K_2 can be expressed in closed-form by evaluating the necessary averages. As an example, the expressions for the coefficients K_0, K_1, and K_2 are presented in Appendix C for the component Ξ_{3333}^{3333}. Explicit expressions for the other 43 independent components are given elsewhere.[45] Traditionally, the Voigt index notation is used to represent the components of the elastic moduli $C_{IJ}^{\text{eff}} = C_{ijkl}^{\text{eff}}$ (see Appendix A for the relation between IJ and $ijkl$). However, it is customary to present the components of $\boldsymbol{\Xi}$ in full index form, $\Xi_{ijkl}^{\alpha\beta\delta\gamma}$. The forthcoming analysis will follow these conventions.

Calculations of the coefficients allow for a straightforward comparison between different polycrystalline materials and tensor components. For example, by using the experimental values of the single-crystal elastic constants located in Table I, the coefficients L_0 and L_1 are given in Tables II and III for polycrystalline iron and aluminum, respectively. It is observed, by comparing the values of L_1, that the component $\langle C_{33}^{\text{eff}} \rangle$ is more sensitive than $\langle C_{11}^{\text{eff}} \rangle$ to the uniaxial stress for both materials.

The coefficients K_0, K_1, and K_2, which define the 44 independent components of $\boldsymbol{\Xi}$, are given in Tables IV and V. Components of $\boldsymbol{\Xi}$ with indices $i = \alpha$, $j = \beta$, $k = \gamma$, and $l = \delta$ define the variability of C_{ijkl}^{eff} throughout the polycrystal.[47] When the indices differ, $\boldsymbol{\Xi}$ is a measure of covariance between C_{ijkl}^{eff} and $C_{\alpha\beta\gamma\delta}^{\text{eff}}$. The components Ξ_{ijkl}^{ijkl}, where no summation is implied over repeated indices, can be used to display the normally distributed elastic constants C_{ijkl}^{eff},

$$f\left(C_{ijkl}^{\text{eff}}, \langle C_{ijkl}^{\text{eff}} \rangle, \Xi_{ijkl}^{ijkl}\right) = \frac{1}{\sqrt{2\pi \Xi_{ijkl}^{ijkl}}} \exp\left[-\frac{(C_{ijkl}^{\text{eff}} - \langle C_{ijkl}^{\text{eff}} \rangle)^2}{2\Xi_{ijkl}^{ijkl}} \right]$$
$$= \frac{1}{\sqrt{2\pi \Xi_{ijkl}^{ijkl}}} \exp\left[-\frac{\left(\delta C_{ijkl}^{\text{eff}}\right)^2}{2\Xi_{ijkl}^{ijkl}} \right]. \quad (26)$$

The function $f(C_{ijkl}^{\text{eff}}, \langle C_{ijkl}^{\text{eff}} \rangle, \Xi_{ijkl}^{ijkl})$ defines the probability that a particular grain has the value C_{ijkl}^{eff}. As an example, Fig. 1

TABLE III. Stress-dependent elastic moduli for aluminum defined in terms of the coefficients L_0 (GPa) and L_1 (dimensionless).

	$\langle C_{11}^{\text{eff}} \rangle$	$\langle C_{12}^{\text{eff}} \rangle$	$\langle C_{13}^{\text{eff}} \rangle$	$\langle C_{33}^{\text{eff}} \rangle$	$\langle C_{44}^{\text{eff}} \rangle$	$\langle C_{66}^{\text{eff}} \rangle$
L_0	111	59.0	59.0	111	26	26
L_1	1.6853	0.1949	−1.1390	−9.8597	−0.7241	0.7452

TABLE IV. Stress-dependent covariance tensor components for iron (single-crystal elastic constants given in Table I) defined in terms of the coefficients K_0 (GPa^2), K_1 (GPa), and K_2 (dimensionless).

	Ξ^{1111}_{1111}	Ξ^{1122}_{1111}	Ξ^{1133}_{1111}	Ξ^{1212}_{1111}	Ξ^{1313}_{1111}	Ξ^{2222}_{1111}	Ξ^{2233}_{1111}	Ξ^{2323}_{1111}	Ξ^{3333}_{1111}	Ξ^{1112}_{1112}	Ξ^{1222}_{1112}
K_0	563.69	−281.84	−281.84	−281.84	−281.84	211.38	70.46	70.46	211.38	352.30	−264.23
K_1	−23.27	28.98	−8.16	33.02	−6.82	−28.76	0.40	−4.99	9.61	−29.57	30.95
K_2	3.14	−1.10	−2.08	−0.99	−2.11	0.87	0.22	0.14	1.92	1.55	−0.99
	Ξ^{1233}_{1112}	Ξ^{1323}_{1112}	Ξ^{1113}_{1113}	Ξ^{1223}_{1113}	Ξ^{1322}_{1113}	Ξ^{1333}_{1113}	Ξ^{1122}_{1122}	Ξ^{1133}_{1122}	Ξ^{1212}_{1122}	Ξ^{1313}_{1122}	Ξ^{3333}_{1122}
K_0	−88.08	−88.08	352.30	−88.08	−88.08	−264.23	317.07	−35.23	317.07	−35.23	70.46
K_1	−2.14	−0.46	2.40	9.84	4.80	−9.50	−31.58	2.30	−30.24	1.62	−3.98
K_2	−0.57	−0.56	2.35	−0.95	−0.20	−2.20	1.40	−0.28	1.29	−0.22	0.50
	Ξ^{1123}_{1123}	Ξ^{1213}_{1123}	Ξ^{2333}_{1123}	Ξ^{1133}_{1133}	Ξ^{1212}_{1133}	Ξ^{1313}_{1133}	Ξ^{2233}_{1133}	Ξ^{2323}_{1133}	Ξ^{3333}_{1133}	Ξ^{1212}_{1212}	Ξ^{1313}_{1212}
K_0	176.15	176.15	−88.08	317.07	−35.23	317.07	−35.23	−35.23	−281.84	317.07	−35.23
K_1	−6.89	−5.20	1.32	8.63	−3.09	7.96	−3.00	3.06	−8.08	−28.89	−3.76
K_2	0.88	0.83	−0.66	2.40	−0.33	2.37	0.05	0.13	−2.47	1.40	−0.38
	Ξ^{3333}_{1212}	Ξ^{1213}_{1213}	Ξ^{2333}_{1213}	Ξ^{1233}_{1233}	Ξ^{1323}_{1233}	Ξ^{1313}_{1313}	Ξ^{2323}_{1313}	Ξ^{3333}_{1313}	Ξ^{1323}_{1323}	Ξ^{1333}_{1333}	Ξ^{3333}_{3333}
K_0	70.46	176.15	−88.08	176.15	176.15	317.07	−35.23	−281.84	−176.15	352.30	563.69
K_1	6.79	−3.52	−5.41	5.81	2.45	7.28	9.12	−13.47	−0.92	11.35	21.08
K_2	0.71	0.90	−0.77	1.17	1.12	2.45	0.20	−2.57	1.13	2.91	5.02

gives the normal distributions $f(C^{\text{eff}}_{33}, \langle C^{\text{eff}}_{33}\rangle, \Xi^{3333}_{3333})$ for different levels of uniaxial stress. For each curve, the most probable value of C^{eff}_{33} is $\langle C^{\text{eff}}_{33}\rangle$. The quantity $\sqrt{\Xi^{3333}_{3333}}$ is the standard deviation of C^{eff}_{33}, which defines the width of each curve. Figure 1 clearly shows how $\langle C^{\text{eff}}_{33}\rangle$ and Ξ^{3333}_{3333} change as a function of uniaxial stress. As the uniaxial stress changes from −500 MPa compression to 500 MPa tension, the width of the normal distribution $(2\sqrt{\Xi^{3333}_{3333}})$ decreases. This decrease indicates that the stress causes the values of C^{eff}_{33} for particular grains to be closer to the mean, $\langle C^{\text{eff}}_{33}\rangle$. As $\Xi^{3333}_{3333} \to 0$, the stress causes the grains to become effectively isotropic. Similar distributions can be generated using the other variance components of $\boldsymbol{\Xi}$.

A comparison made between $\langle \mathbf{C}^{\text{eff}}\rangle$ and $\boldsymbol{\Xi}$ is important when considering applications in ultrasonic nondestructive evaluation because both tensors help define experimentally measurable parameters. The stress-dependence of $\langle \mathbf{C}^{\text{eff}}\rangle$ indicates the sensitivity of the phase velocity for a small-amplitude ultrasonic wave to the material stress state. For example, when a compressional wave propagates parallel to the uniaxial stress, σ_{33}, the phase velocity is given by $V_L = (\langle C^{\text{eff}}_{33}\rangle/\rho)^{1/2}$ whereas a compressional wave propagating perpendicular to the uniaxial stress is $V_L = (\langle C^{\text{eff}}_{11}\rangle/\rho)^{1/2}$. Similarly, the component Ξ^{3333}_{3333} dictates the intensity of ultrasonic grain scattering when

TABLE V. Stress-dependent covariance tensor components for aluminum (single-crystal elastic constants given in Table I) defined in terms of the coefficients K_0 (GPa^2), K_1 (GPa), and K_2 (dimensionless).

	Ξ^{1111}_{1111}	Ξ^{1122}_{1111}	Ξ^{1133}_{1111}	Ξ^{1212}_{1111}	Ξ^{1313}_{1111}	Ξ^{2222}_{1111}	Ξ^{2233}_{1111}	Ξ^{2323}_{1111}	Ξ^{3333}_{1111}	Ξ^{1112}_{1112}	Ξ^{1222}_{1112}
K_0	3.048	−1.524	−1.524	−1.524	−1.524	1.143	0.381	0.381	1.143	1.905	−1.429
K_1	1.161	−0.798	0.038	−0.714	0.065	0.597	0.10	−0.011	−0.438	0.847	−0.706
K_2	0.907	−0.197	−0.655	−0.187	−0.650	0.103	0.075	0.059	0.544	0.370	−0.169
	Ξ^{1233}_{1112}	Ξ^{1323}_{1112}	Ξ^{1113}_{1113}	Ξ^{1223}_{1113}	Ξ^{1322}_{1113}	Ξ^{1333}_{1113}	Ξ^{1122}_{1122}	Ξ^{1133}_{1122}	Ξ^{1212}_{1122}	Ξ^{1313}_{1122}	Ξ^{3333}_{1122}
K_0	−0.476	−0.476	1.905	−0.476	−0.476	−1.429	1.714	−0.190	1.714	−0.190	0.381
K_1	−0.016	0.019	−0.016	−0.032	−0.137	0.528	0.751	0.098	0.779	0.084	−0.295
K_2	−0.183	−0.178	0.753	−0.037	−0.034	−0.729	0.298	−0.115	0.291	−0.111	0.256
	Ξ^{1123}_{1123}	Ξ^{1213}_{1123}	Ξ^{2333}_{1123}	Ξ^{1133}_{1133}	Ξ^{1212}_{1133}	Ξ^{1313}_{1133}	Ξ^{2233}_{1133}	Ξ^{2323}_{1133}	Ξ^{3333}_{1133}	Ξ^{1212}_{1212}	Ξ^{1313}_{1212}
K_0	0.952	0.952	−0.476	1.714	−0.190	1.714	−0.190	−0.190	−1.524	1.714	−0.190
K_1	−0.007	0.027	0.269	−0.585	−0.014	−0.599	−0.148	−0.023	1.133	0.806	−0.028
K_2	0.281	0.273	−0.275	0.847	−0.088	0.841	0.059	0.037	−1.002	0.300	−0.092
	Ξ^{3333}_{1212}	Ξ^{1213}_{1213}	Ξ^{2333}_{1213}	Ξ^{1233}_{1233}	Ξ^{1323}_{1233}	Ξ^{1313}_{1313}	Ξ^{2323}_{1313}	Ξ^{3333}_{1313}	Ξ^{1323}_{1323}	Ξ^{1333}_{1333}	Ξ^{3333}_{3333}
K_0	0.381	0.952	−0.476	0.952	0.952	1.714	−0.190	−1.524	0.952	1.905	3.048
K_1	−0.072	0.062	0.129	−0.218	−0.288	−0.613	0.103	1.022	−0.358	−1.297	−3.066
K_2	0.144	0.275	−0.227	0.394	0.402	0.845	0.015	−0.946	0.415	1.174	2.406

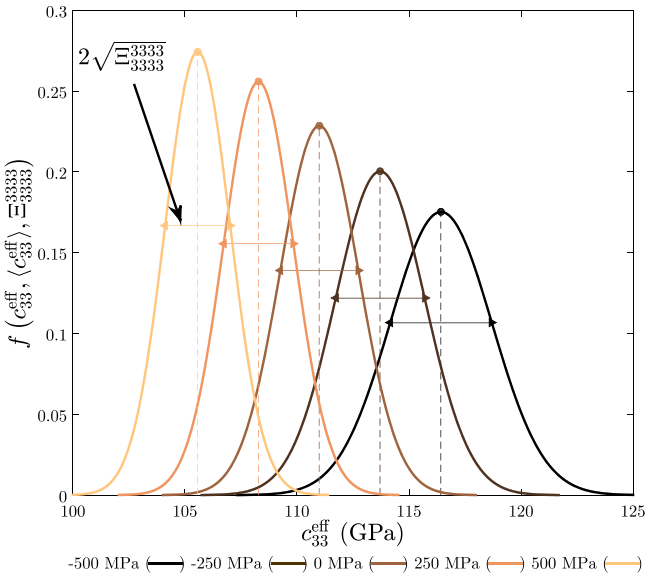

FIG. 1. (Color online) The probability distribution function defining the likelihood that c^{eff}_{33} for a single-grain obtains one of the distribution of values. Each curve is normally distributed about the peak value of $\langle c^{\text{eff}}_{33}\rangle$. The different curves represent the influence of the uniaxial stress on the aluminum polycrystal. Moving from values of compression to large values of tension, the variance tensor Ξ^{3333}_{3333} (or the square of the standard deviation) becomes smaller. Thus, for this example, the uniaxial stress causes a decrease in variability of c^{eff}_{33} amongst the ensemble of grains.

considering an incident wave parallel to the uniaxial stress that scatters backwards in the opposite direction.[1,2] The influence of uniaxial stress on backscatter, which was perpendicular to the uniaxial stress, was considered experimentally by Kube *et al.*[18] In this case, the change in the backscatter amplitude was caused by the sensitivity of the component Ξ^{1111}_{1111} to the uniaxial stress. Other scattering configurations where the incident wave is scattered into an arbitrary direction are dependent on other components of $\Xi^{\alpha\beta\gamma\delta}_{ijkl}$.[48–50] Additionally, other scattering related phenomenon such as ultrasonic attenuation[21–25,51] and radiative transfer of ultrasound[48,52–54] depend on inner products with $\boldsymbol{\Xi}$. The stress-dependence of each of these models is included by using the definition of $\boldsymbol{\Xi}$ defined in this article.

The stress-dependence of $\langle C^{\text{eff}}_{ijkl}\rangle$ and Ξ^{ijkl}_{ijkl} is illustrated in Figs. 2 and 3 for iron and aluminum, respectively. Figures 2 and 3 illustrate that $\boldsymbol{\Xi}$ has a much greater sensitivity to the uniaxial stress than $\langle \mathbf{C}^{\text{eff}}\rangle$. This result indicates that many measurable quantities related to ultrasonic scattering have the potential to have much greater measurement resolution than previous acoustoelastic techniques based on phase velocity measurements. For aluminum, the sensitivity of $\boldsymbol{\Xi}$ is greater than iron partly because of the strong quadratic dependence, which depends on the second-order coefficient K_2. The underlying cause of the increased sensitivity of aluminum compared with iron arises from the magnitudes of the single-crystal elastic anisotropy constants ν, d_1, d_2, and d_3.

The relation between the stresses in a polycrystalline material and scattering based measurements has a strong potential for development into techniques for stress evaluation. Alternatively, neglecting the possible stresses when applying scattering based techniques to measure other variables could introduce severe errors into the measurement. For example, several researchers[1–4,6–10] use ultrasonic grain noise as a measurement tool of the microstructural grain dimensions. If the measurements were done on samples with large residual stress levels, their resultant grain dimension measurements are likely incorrect estimates. An error in other measurement parameters, such as macroscopic texture,[12,13] could also be considerable.

IV. CONCLUSION

In this article, the stress-dependence of the covariance tensor $\boldsymbol{\Xi}$ was derived. This tensor is a measure of the variability of the elastic constants throughout the polycrystal. To arrive at $\boldsymbol{\Xi}$, the stress-dependent effective elastic modulus for a single crystallite was defined as $\mathbf{C}^{\text{eff}}$, which is homogenized in order to define the analogous tensor $\langle \mathbf{C}^{\text{eff}}\rangle$. $\langle \mathbf{C}^{\text{eff}}\rangle$ is the stress-dependent effective elastic modulus tensor for a stressed polycrystal. The definition of $\boldsymbol{\Xi}$ differs from the previous definition in Turner and Ghoshal[17] by making use of the constitutive stress/strain relation developed by Man and co-workers and Huang *et al.*[31–37] This constitutive relation introduces the initial stress $\boldsymbol{\sigma}$, which is valid for residual or mechanically induced stresses.

An evaluation of the components of $\boldsymbol{\Xi}$ demonstrates the strong dependence on the stresses in the material. This stress-dependency can cause the elastic moduli of individual grains to deviate or converge toward the mean value, $\langle \mathbf{C}^{\text{eff}}\rangle$. The stressed-induced variations of $\mathbf{C}^{\text{eff}}$, which is governed by $\boldsymbol{\Xi}$, amongst the grains strongly influences ultrasonic scattering based phenomenon. The stronger stress sensitivity of $\boldsymbol{\Xi}$ compared to $\langle \mathbf{C}^{\text{eff}}\rangle$ indicates that scattering based methods could be preferred over phase velocity techniques for nondestructive stress analysis.

The influence of stresses on $\boldsymbol{\Xi}$ also impacts model-assisted scattering measurements where the material stresses have been neglected previously. Common parameters

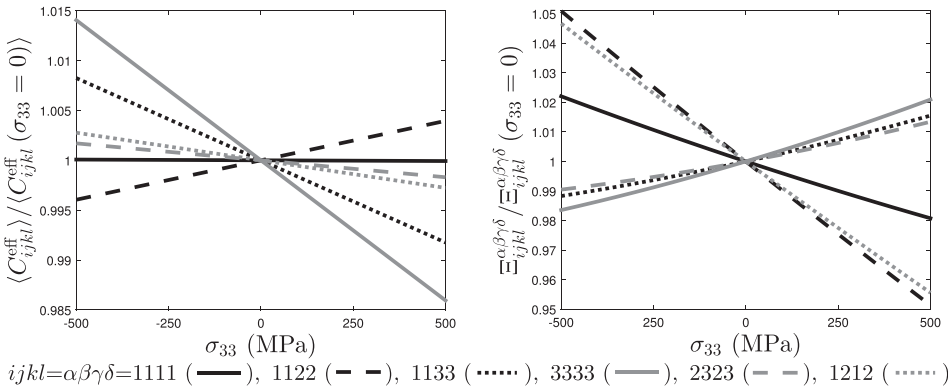

FIG. 2. The effective stress-dependent elastic moduli $\langle C^{\text{eff}}_{ijkl}\rangle$ and stress-dependent covariance tensor $\Xi^{\alpha\beta\gamma\delta}_{ijkl}$ for iron normalized to their stress-free values plotted against values of uniaxial stress. The curves were generated using the data from Tables II and IV and single-crystal elastic constants from Table I.

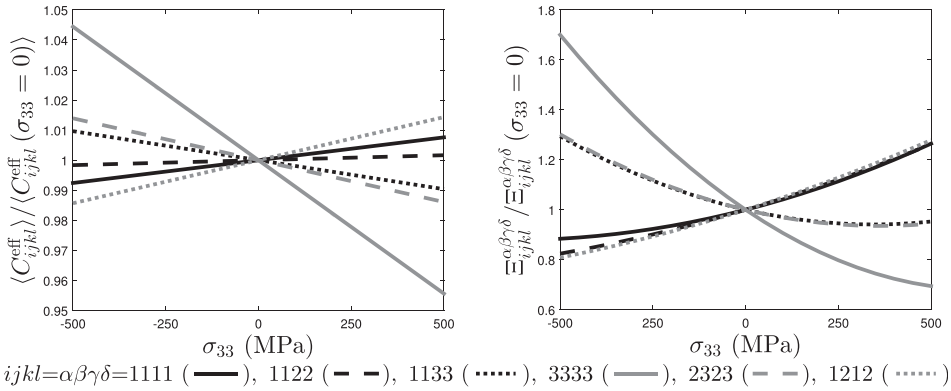

FIG. 3. The effective stress-dependent elastic moduli $\langle C^{\mathrm{eff}}_{ijkl}\rangle$ and stress-dependent covariance tensor $\Xi^{\alpha\beta\gamma\delta}_{ijkl}$ for aluminum normalized to their stress-free values plotted against values of uniaxial stress. The curves were generated using the data from Tables III and V and single-crystal elastic constants from Table I.

measured by ultrasonic scattering such as grain dimensions or material texture could contain large errors if the experimental samples contained residual stresses.

This theory forms the starting point of an acoustoelastic description of wave propagation and scattering in polycrystalline materials. Future work will focus on using the stress-dependent elastic properties $\mathbf{C}^{\mathrm{eff}}$, $\langle \mathbf{C}^{\mathrm{eff}} \rangle$, and $\boldsymbol{\Xi}$ to arrive at explicit stress-dependent models for scattering related phenomenon.

ACKNOWLEDGMENTS

The support of the Federal Railroad Administration (Grant No. DTFR53-G-00011) for this research is gratefully acknowledged.

APPENDIX A: TENSOR DEFINITIONS FOR THE SECOND- AND THIRD-ORDER ELASTIC CONSTANTS OF CRYSTALS

The elastic fourth- and sixth-rank tensors defining the elastic moduli are C_{ijkl} and C_{ijklmn}, respectively. Both tensors exhibit the minor ($C_{ijkl}=C_{jikl}=C_{ijlk}$, $C_{ijklmn}=C_{jiklmn}=C_{ijklkmn}=C_{ijklnm}$) and major ($C_{ijkl}=C_{klij}$, $C_{ijklmn}=C_{klijmn}=C_{mnklij}$) symmetries, which reduces the number of independent second- and third-order elastic constants to 21 and 56, respectively. The fourth-rank tensor defining the elastic compliance is S_{ijkl} and exhibits the same symmetries as C_{ijkl}. These tensors can be written with respect to a rotated Cartesian coordinate system using the transformations[55]

$$C'_{ijkl} = a_{ip}a_{jq}a_{kr}a_{ls}C_{pqrs}, \quad S'_{ijkl} = a_{ip}a_{jq}a_{kr}a_{ls}S_{pqrs}, \text{ and}$$
$$C'_{ijklmn} = a_{ip}a_{jq}a_{kr}a_{ls}a_{mt}a_{nu}C_{pqrstu}, \tag{A1}$$

where a_{ij} are components of the transformation matrix and the primed notation is used to describe the tensors in the rotated system. Expansion of the tensors in Eq. (A1) and application of the major and minor elastic symmetry relations gives general forms of the tensors for any rotated coordinate system. Such forms are appropriate to describe the elastic properties of grains with various orientations. The general forms of Eq. (A1) can be simplified using the symmetry relations for specific crystallographic point groups.[56] For example, the expansion of C_{ijkl} in Eq. (A1) for cubic crystals is

$$\begin{aligned} C_{ijkl} = {} & c_{11}(a_{i1}a_{j1}a_{k1}a_{l1} + a_{i2}a_{j2}a_{k2}a_{l2} + a_{i3}a_{j3}a_{k3}a_{l3}) + c_{12}(a_{i1}a_{j1}a_{k2}a_{l2} + a_{i2}a_{j2}a_{k1}a_{l1} \\ & + a_{i1}a_{j1}a_{k3}a_{l3} + a_{i3}a_{j3}a_{k1}a_{l1} + a_{i2}a_{j2}a_{k3}a_{l3} + a_{i3}a_{j3}a_{k2}a_{l2}) \\ & + c_{44}(a_{i1}a_{j2}a_{k1}a_{l2} + a_{i1}a_{j2}a_{k2}a_{l1} + a_{i2}a_{j1}a_{k1}a_{l2} + a_{i2}a_{j1}a_{k2}a_{l1} + a_{i1}a_{j3}a_{k1}a_{l3} \\ & + a_{i1}a_{j3}a_{k3}a_{l1} + a_{i3}a_{j1}a_{k1}a_{l3} + a_{i3}a_{j1}a_{k3}a_{l1} + a_{i2}a_{j3}a_{k2}a_{l3} + a_{i2}a_{j3}a_{k3}a_{l2} \\ & + a_{i3}a_{j2}a_{k2}a_{l3} + a_{i3}a_{j2}a_{k3}a_{l2}), \end{aligned} \tag{A2}$$

where the Voigt index notation has been utilized (index pairs $11 \rightarrow 1$, $22 \rightarrow 2$, $33 \rightarrow 3$, $23 \rightarrow 4$, $13 \rightarrow 5$, $12 \rightarrow 6$) along with the symmetry relations $c_{11}=c_{22}=c_{33}$, $c_{12}=c_{13}=c_{23}$, $c_{44}=c_{55}=c_{66}$. Making use of the identity $a_{iu}a_{ju}=\delta_{ij}$, Eq. (A2) can be simplified to

$$C_{ijkl} = c_{12}\delta_{ij}\delta_{kl} + 2c_{44}I_{ijkl} + \nu A_{ijkl}, \tag{A3}$$

where $A_{ijkl}=a_{iu}a_{ju}a_{ku}a_{lu}$ and $\nu = c_{11}-c_{12}-2c_{44}$ is the anisotropy coefficient for the second-order elastic constants of cubic crystals. Equation (A3) was first derived by Thomas who sought an invariant form of Hooke's law for crystals of cubic symmetry.[57] The fourth-rank elastic compliance tensor for cubic crystals can be written immediately as

$$S_{ijkl} = s_{12}\delta_{ij}\delta_{kl} + 2s_{44}I_{ijkl} + \nu_s A_{ijkl}, \tag{A4}$$

where $\nu_s = s_{11}-s_{12}-2s_{44}$. Equations (A3) and (A4) can be shown to satisfy the relation $C_{ijmn}S_{mnkl}=I_{ijkl}$, from which the relations between elastic constants and compliances can be obtained for any crystallographic symmetry. For crystals of cubic symmetry

$$s_{11} = \frac{c_{11}+c_{12}}{(c_{11}-c_{12})(c_{11}+2c_{12})},$$
$$s_{12} = -\frac{c_{12}}{(c_{11}-c_{12})(c_{11}+2c_{12})}, \quad s_{44} = \frac{1}{4c_{44}}. \tag{A5}$$

An incorrect stiffness/compliance relation, $s_{44} = 1/c_{44}$, was used in the previous work of Turner and Ghoshal.[17] Equation (A5) gives the correction to this error. An analogous procedure is used to obtain a simplified general form of the sixth-rank tensor C_{ijklmn} for cubic crystals, which is given as

$$C_{ijklmn} = c_{123}\delta^1_{ijklmn} + 2c_{144}\delta^2_{ijklmn} + 2c_{456}\delta^3_{ijklmn} + d_1 A^1_{ijklmn} + d_2 A^2_{ijklmn} + d_3 A^3_{ijklmn}, \tag{A6}$$

where $d_1 = c_{111} - 3c_{112} + 2c_{123} + 12c_{144} - 12c_{155} + 16c_{456}$, $d_2 = c_{112} - c_{123} - 2c_{144}$, and $d_3 = c_{155} - c_{144} - 2c_{456}$ are the three anisotropy constants of the third-order elastic constants. The first three terms of C_{ijklmn} are given as a linear combination of the three sixth-rank isotropic tensors,

$$\delta^1_{ijklmn} = \delta_{ij}\delta_{kl}\delta_{mn}, \quad \delta^2_{ijklmn} = \delta_{ij}I_{klmn} + \delta_{kl}I_{ijmn} + \delta_{mn}I_{ijkl},$$
$$\delta^3_{ijklmn} = \delta_{ik}I_{jlmn} + \delta_{il}I_{jkmn} + \delta_{im}I_{jnkl} + \delta_{in}I_{jklm}, \tag{A7}$$

while the last three terms are given as

$$\begin{aligned} A^1_{ijklmn} &= a_{iu}a_{ju}a_{ku}a_{lu}a_{mu}a_{nu}, \\ A^2_{ijklmn} &= \delta_{ij}A_{klmn} + \delta_{kl}A_{ijmn} + \delta_{mn}A_{ijkl}, \text{ and} \\ A^3_{ijklmn} &= \delta_{ik}A_{jlmn} + \delta_{il}A_{klmn} + \delta_{im}A_{jkln} + \delta_{in}A_{jklm} \\ &\quad + \delta_{jk}A_{ilmn} + \delta_{jl}A_{ikmn} + \delta_{jm}A_{ikln} + \delta_{jn}A_{iklm} \\ &\quad + \delta_{km}A_{ijln} + \delta_{kn}A_{ijlm} + \delta_{lm}A_{ijkn} + \delta_{ln}A_{ijkm}. \end{aligned} \tag{A8}$$

Equation (A6) agrees with the expressions given by Barsch[58] and Ballabh *et al.*[59] The construction of invariant tensors of higher rank can proceed in the same manner.

It is often convenient to write C_{ijkl} and C_{ijklmn} in terms of isotropic and orientation dependent parts

$$C_{ijkl} = C^I_{ijkl} + C^A_{ijkl}, \; C_{ijklmn} = C^I_{ijklmn} + C^A_{ijklmn}, \tag{A9}$$

where

$$\begin{aligned} C^I_{ijkl} &= c_{12}\delta_{ij}\delta_{kl} + 2c_{44}I_{ijkl}, \quad C^A_{ijkl} = \nu A_{ijkl}, \\ C^I_{ijklmn} &= c_{123}\delta^1_{ijklmn} + 2c_{144}\delta^2_{ijklmn} + 2c_{456}\delta^3_{ijklmn}, \text{ and} \\ C^A_{ijklmn} &= d_1 A^1_{ijklmn} + d_2 A^2_{ijklmn} + d_3 A^3_{ijklmn}. \end{aligned} \tag{A10}$$

These definitions help simplify the expressions and computational burden when calculating the covariance tensors in Eq. (24).

APPENDIX B: TENSOR AVERAGES

The computational demands of the orientation averages are greatly reduced by the physical assumption of randomly oriented grains. For such a case, all averages of the orientation dependent tensors can be written as isotropic tensors. Even-rank isotropic tensors up to Nth-rank can be obtained using an iteration procedure given by[60,61]

$$I^{(N)}_{i_1\ldots i_N} = \delta_{i_1 i_2} I^{(N-2)}_{i_3 i_4 i_5 i_6 \ldots i_N} + \delta_{i_1 i_3} I^{(N-2)}_{i_2 i_4 i_5 i_6 \ldots i_N} + \delta_{i_1 i_4} I^{(N-2)}_{i_2 i_3 i_5 i_6 \ldots i_N} + \cdots + (N-1 \text{ terms}), \tag{B1}$$

for $N = 2$ to 12,

$$\begin{aligned} I^{(2)}_{ij} &= \delta_{ij}, \\ I^{(4)}_{ijkl} &= \delta_{ij}I^{(2)}_{kl} + \delta_{ik}I^{(2)}_{jl} + \delta_{il}I^{(2)}_{jk}, \\ I^{(6)}_{ijklmn} &= \delta_{ij}I^{(4)}_{klmn} + \delta_{ik}I^{(4)}_{jlmn} + \delta_{il}I^{(4)}_{jkmn} + \delta_{im}I^{(4)}_{jkln} + \delta_{in}I^{(4)}_{jklm}, \\ I^{(8)}_{ijklkmnpq} &= \delta_{ij}I^{(6)}_{klmnpq} + \delta_{ik}I^{(6)}_{jlmnpq} + \delta_{il}I^{(6)}_{jkmnpq} + \delta_{im}I^{(6)}_{jklnpq} \\ &\quad + \delta_{in}I^{(6)}_{jklmpq} + \delta_{ip}I^{(6)}_{jklmnq} + \delta_{iq}I^{(6)}_{jklmnp}, \\ I^{(10)}_{ijklmnpqrs} &= \delta_{ij}I^{(8)}_{klmnpqrs} + \delta_{ik}I^{(8)}_{jlmnpqrs} + \delta_{il}I^{(8)}_{jkmnpqrs} \\ &\quad + \delta_{im}I^{(8)}_{jklnpqrs} + \delta_{in}I^{(8)}_{jklmpqrs} + \delta_{ip}I^{(8)}_{jklmnqrs} \\ &\quad + \delta_{iq}I^{(8)}_{jklmnprs} + \delta_{ir}I^{(8)}_{jklmnpqs} + \delta_{is}I^{(8)}_{jklmnpqr}, \\ I^{(12)}_{ijklmnpqrstw} &= \delta_{ij}I^{(10)}_{klmnpqrstw} + \delta_{ik}I^{(10)}_{jlmnpqrstw} + \delta_{il}I^{(10)}_{jkmnpqrstw} \\ &\quad + \delta_{im}I^{(10)}_{jklnpqrstw} + \delta_{in}I^{(10)}_{jklmpqrstw} + \delta_{ip}I^{(10)}_{jklmnqrstw} \\ &\quad + \delta_{iq}I^{(10)}_{jklmnprstw} + \delta_{ir}I^{(10)}_{jklmnpqstw} + \delta_{is}I^{(10)}_{jklmnpqrtw} \\ &\quad + \delta_{it}I^{(10)}_{jklmnpqrsw} + \delta_{iw}I^{(10)}_{jklmnpqrst}, \end{aligned} \tag{B2}$$

where the number of summed terms in the Nth-rank tensor is $1 \times 3 \times 5 \times \cdots \times (N-1)$. As an example, the averages needed to calculate $\langle C_{ijkl}\rangle$ and $\langle C_{ijklmn}\rangle$ are

$$\langle a_{iu}a_{ju}a_{ku}a_{lu}\rangle = \frac{1}{5}I^{(4)}_{ijkl},$$
$$\langle a_{iu}a_{ju}a_{ku}a_{lu}a_{mu}a_{nu}\rangle = \frac{1}{35}I^{(6)}_{ijklmn}. \tag{B3}$$

Higher-rank averages are more complex but can also be written in terms of the isotropic tensors

$$\begin{aligned} &\langle a_{iu}a_{ju}a_{ku}a_{lu}a_{\alpha v}a_{\beta v}a_{\gamma v}a_{\delta v}\rangle \\ &\quad = \frac{4}{105}I_{LLLLGGGG} + \frac{1}{420}I_{LGLGLGLG} + \frac{13}{35}I_{LLGGLGLG}, \\ &\langle a_{iu}a_{ju}a_{ku}a_{lu}a_{\alpha v}a_{\beta v}a_{\gamma v}a_{\delta v}a_{\epsilon v}a_{\zeta v}\rangle \\ &\quad = \frac{1}{165}I_{LLLLGGGGGG} - \frac{1}{3465}I_{LLGGGGLGLG} \\ &\qquad + \frac{1}{1980}I_{GGLGLGLGLG}, \\ &\langle a_{iu}a_{ju}a_{ku}a_{lu}a_{mu}a_{nu}a_{\alpha v}a_{\beta v}a_{\gamma v}a_{\delta v}\rangle \\ &\quad = \frac{1}{165}I_{LLLLLLGGGG} - \frac{1}{3465}I_{LLLLGGLGLG} \\ &\qquad + \frac{1}{1980}I_{LLLGLGLGLG}, \\ &\langle a_{iu}a_{ju}a_{ku}a_{lu}a_{mu}a_{nu}a_{\alpha v}a_{\beta v}a_{\gamma v}a_{\delta v}a_{\epsilon v}a_{\zeta v}\rangle \\ &\quad = \frac{41}{45045}I_{LLLLLLGGGGGG} - \frac{1}{19305}I_{LLLLGGGGLGLG} \\ &\qquad + \frac{2}{45045}I_{LLGGLGLGLGLG} + \frac{1}{120120}I_{LGLGLGLGLGLG}, \end{aligned} \tag{B4}$$

where

$$
\begin{aligned}
I_{LLLLGGGG} &= I^{(4)}_{ijkl} I^{(4)}_{\alpha\beta\gamma\delta} \\
&= \delta_{ij}\delta_{kl}\delta_{\alpha\beta}\delta_{\gamma\delta} + \text{all permutations of two pairs of Latin and} \\
&\quad \text{Latin indices, and two pairs of Greek and Greek indices (9 terms)}, \\
I_{LGLGLGLG} &= \delta_{i\alpha}\delta_{j\beta}\delta_{k\gamma}\delta_{l\delta} + \text{all permutations of four pairs of Latin and Greek indices (24 terms)}, \\
I_{LLGGLGLG} &= \delta_{ij}\delta_{\alpha\beta}\delta_{k\gamma}\delta_{l\delta} + \text{all permutations of two pairs of Latin and Greek indices,} \\
&\quad \text{one pair of Latin and Latin indices, and one pair of Greek and Greek indices (72 terms)}, \\
I_{LLLLGGGGGG} &= I^{(4)}_{ijkl} I^{(6)}_{\alpha\beta\gamma\delta\epsilon\zeta} \\
&= \delta_{ij}\delta_{kl}\delta_{\alpha\beta}\delta_{\gamma\delta}\delta_{\epsilon\zeta} + \text{all permutations of two pairs of Latin and} \\
&\quad \text{Latin indices, and three pairs of Greek and Greek indices (45 terms)}, \\
I_{LLGGGGLGLG} &= \delta_{ij}\delta_{\alpha\beta}\delta_{\gamma\delta}\delta_{k\epsilon}\delta_{l\zeta} + \text{all permutations of one pair of Latin and} \\
&\quad \text{Latin indices, two pairs of Greek and Greek indices, and two pairs of} \\
&\quad \text{Latin and Greek indices (540 terms)}, \\
I_{LLLGLGLGLG} &= \delta_{ij}\delta_{k\alpha}\delta_{l\beta}\delta_{m\gamma}\delta_{n\delta} + \text{all permutations of one pair of Latin and} \\
&\quad \text{Latin indices, and four pairs of Latin and Greek indices (360 terms)}, \\
I_{LLLLLLGGGG} &= I^{(6)}_{ijklmn} I^{(4)}_{\alpha\beta\gamma\delta} \\
&= \delta_{ij}\delta_{kl}\delta_{mn}\delta_{\alpha\beta}\delta_{\gamma\delta} + \text{all permutations of three pairs of Latin and} \\
&\quad \text{Latin indices, and two pairs of Greek and Greek indices (45 terms)}, \\
I_{LLLLGGLGLG} &= \delta_{ij}\delta_{kl}\delta_{\alpha\beta}\delta_{m\gamma}\delta_{n\delta} + \text{all permutations of two pairs of Latin and} \\
&\quad \text{Latin indices, one pair of Greek and Greek indices, and two pairs of} \\
&\quad \text{Latin and Greek indices (540 terms)}, \\
I_{GGLGLGLGLG} &= \delta_{\alpha\beta}\delta_{i\gamma}\delta_{j\delta}\delta_{k\epsilon}\delta_{l\zeta} + \text{all permutations of one pair of Greek and} \\
&\quad \text{Greek indices, and four pairs of Latin and Greek indices (360 terms)}, \\
I_{LLLLLLGGGGGG} &= I^{(6)}_{ijklmn} I^{(6)}_{\alpha\beta\gamma\delta\epsilon\zeta} \\
&= \delta_{ij}\delta_{kl}\delta_{mn}\delta_{\alpha\beta}\delta_{\gamma\delta}\delta_{\epsilon\zeta} + \text{all permutations of three pairs of Latin and} \\
&\quad \text{Latin indices, and three pairs of Greek and Greek indices (225 terms)}, \\
I_{LLLLGGGGLGLG} &= \delta_{ij}\delta_{kl}\delta_{\alpha\beta}\delta_{\gamma\delta}\delta_{m\epsilon}\delta_{n\zeta} + \text{all permutations of two pairs of Latin and} \\
&\quad \text{Latin indices, two pairs of Greek and Greek indices, and two pairs of} \\
&\quad \text{Latin and Greek indices (4050 terms)}, \\
I_{LLGGLGLGLGLG} &= \delta_{ij}\delta_{\alpha\beta}\delta_{k\gamma}\delta_{l\delta}\delta_{m\epsilon}\delta_{n\zeta} + \text{all permutations of one pair of Latin and} \\
&\quad \text{Latin indices, one pair of Greek and Greek indices, and four pairs of} \\
&\quad \text{Latin and Greek indices (5400 terms)}, \\
I_{LGLGLGLGLGLG} &= \delta_{i\alpha}\delta_{j\beta}\delta_{k\gamma}\delta_{l\delta}\delta_{m\epsilon}\delta_{n\zeta} + \text{all permutations of six pairs of Latin and Greek indices (720 terms)}.
\end{aligned} \tag{B5}
$$

The 105 terms containing products of 8 Kronecker delta functions are the individual terms found in $I^{(8)}_{ijklmnpq}$, while the 945 terms containing products of 10 delta functions are the individual terms found in $I^{(10)}_{ijklmnpqrs}$, and the 10 395 terms containing products of 12 delta functions are the individual terms found in $I^{(12)}_{ijklmnpqrstw}$.

APPENDIX C: EXAMPLE EXPRESSION FOR THE COMPONENT Ξ^{3333}_{3333}

The individual components of $\boldsymbol{\Xi}$ may be written in terms of the coefficients K_0, K_1, and K_2. Thus, as an example, the analytical form of the component $\Xi^{3333}_{3333} = K_0 + K_1\sigma_{33} + K_2\sigma_{33}^2$, where

$$
\begin{aligned}
K_0 &= \frac{16\nu^2}{525}, \\
K_1 &= \frac{32s_{12}\nu^2}{525} + \frac{64s_{44}\nu^2}{175} + \frac{224\nu^2\nu_s}{825} + \frac{128c_{12}\nu\nu_s}{525} + \frac{256c_{44}\nu\nu_s}{525} + \frac{128c_{144}\nu\nu_s}{525} + \frac{256c_{456}\nu\nu_s}{525} + \frac{32s_{12}d_1\nu}{525} + \frac{32s_{12}d_2\nu}{175} \\
&\quad + \frac{256s_{12}d_3\nu}{525} + \frac{64s_{44}d_1\nu}{385} + \frac{64s_{44}d_2\nu}{175} + \frac{256s_{44}d_3\nu}{175} + \frac{32d_1\nu\nu_s}{385} + \frac{32d_2\nu\nu_s}{175} + \frac{5248d_3\nu\nu_s}{5775}, \text{ and}
\end{aligned}
$$

$$K_2 = \frac{256c_{12}^2\nu_s^2}{525} + \frac{1024c_{44}^2\nu_s^2}{525} + \frac{256c_{144}^2\nu_s^2}{525} + \frac{1024c_{456}^2\nu_s^2}{525} + \frac{16s_{12}^2d_1^2}{525} + \frac{48s_{12}^2d_2^2}{175} + \frac{1024s_{12}^2d_3^2}{525} + \frac{1600s_{44}^2d_1^2}{7007} + \frac{192s_{44}^2d_2^2}{175}$$
$$+ \frac{3072s_{44}^2d_3^2}{175} + \frac{16s_{12}^2\nu^2}{525} + \frac{192s_{44}^2\nu^2}{175} + \frac{400d_1^2\nu_s^2}{7007} + \frac{48d_2^2\nu_s^2}{175} + \frac{3574016d_3^2\nu_s^2}{525525} + \frac{321296\nu^2\nu_s^2}{525525} + \frac{1024c_{12}c_{44}\nu_s^2}{525}$$
$$+ \frac{512c_{12}c_{144}\nu_s^2}{525} + \frac{1024c_{44}c_{144}\nu_s^2}{525} + \frac{1024c_{12}c_{456}\nu_s^2}{525} + \frac{2048c_{44}c_{456}\nu_s^2}{525} + \frac{1024c_{144}c_{456}\nu_s^2}{525} + \frac{64s_{12}s_{44}d_1^2}{385} + \frac{192s_{12}s_{44}d_2^2}{175}$$
$$+ \frac{2048s_{12}s_{44}d_3^2}{175} + \frac{64s_{12}s_{44}\nu^2}{175} + \frac{128c_{12}d_1\nu_s^2}{385} + \frac{128c_{12}d_2\nu_s^2}{175} + \frac{20992c_{12}d_3\nu_s^2}{5775} + \frac{256c_{44}d_1\nu_s^2}{385} + \frac{256c_{44}d_2\nu_s^2}{175}$$
$$+ \frac{41984c_{44}d_3\nu_s^2}{5775} + \frac{128c_{144}d_1\nu_s^2}{385} + \frac{128c_{144}d_2\nu_s^2}{175} + \frac{20992c_{144}d_3\nu_s^2}{5775} + \frac{256c_{456}d_1\nu_s^2}{385} + \frac{256c_{456}d_2\nu_s^2}{175} + \frac{41984c_{456}d_3\nu_s^2}{5775}$$
$$+ \frac{32s_{12}^2d_1d_2}{175} + \frac{256s_{12}^2d_1d_3}{525} + \frac{256s_{12}^2d_2d_3}{175} + \frac{384s_{44}^2d_1d_2}{385} + \frac{1536s_{44}^2d_1d_3}{385} + \frac{1536s_{44}^2d_2d_3}{175} + \frac{896c_{12}\nu\nu_s^2}{825} + \frac{1792c_{44}\nu\nu_s^2}{825}$$
$$+ \frac{896c_{144}\nu\nu_s^2}{825} + \frac{1792c_{456}\nu\nu_s^2}{825} + \frac{32s_{12}^2d_1\nu}{525} + \frac{32s_{12}^2d_2\nu}{175} + \frac{256s_{12}^2d_3\nu}{525} + \frac{384s_{44}^2d_1\nu}{385} + \frac{384s_{44}^2d_2\nu}{175} + \frac{1536s_{44}^2d_3\nu}{175}$$
$$+ \frac{32s_{12}d_1^2\nu_s}{385} + \frac{96s_{12}d_2^2\nu_s}{175} + \frac{41984s_{12}d_3^2\nu_s}{5775} + \frac{1600s_{44}d_1^2\nu_s}{7007} + \frac{192s_{44}d_2^2\nu_s}{175} + \frac{41984s_{44}d_3^2\nu_s}{1925} + \frac{224s_{12}\nu^2\nu_s}{825} + \frac{448s_{44}\nu^2\nu_s}{275}$$
$$+ \frac{96d_1d_2\nu_s^2}{385} + \frac{3968d_1d_3\nu_s^2}{3185} + \frac{5248d_2d_3\nu_s^2}{1925} + \frac{13088d_1\nu\nu_s^2}{35035} + \frac{224d_2\nu\nu_s^2}{275} + \frac{2141312d_3\nu\nu_s^2}{525525} + \frac{128c_{12}s_{12}d_1\nu_s}{525}$$
$$+ \frac{128c_{12}s_{12}d_2\nu_s}{175} + \frac{1024c_{12}s_{12}d_3\nu_s}{525} + \frac{256c_{12}s_{44}d_1\nu_s}{385} + \frac{256c_{44}s_{12}d_1\nu_s}{525} + \frac{256c_{12}s_{44}d_2\nu_s}{175} + \frac{256c_{44}s_{12}d_2\nu_s}{175}$$
$$+ \frac{1024c_{12}s_{44}d_3\nu_s}{175} + \frac{2048c_{44}s_{12}d_3\nu_s}{525} + \frac{512c_{44}s_{44}d_1\nu_s}{385} + \frac{512c_{44}s_{44}d_2\nu_s}{175} + \frac{2048c_{44}s_{44}d_3\nu_s}{175} + \frac{128c_{144}s_{12}d_1\nu_s}{525}$$
$$+ \frac{128c_{144}s_{12}d_2\nu_s}{175} + \frac{1024c_{144}s_{12}d_3\nu_s}{525} + \frac{256c_{144}s_{44}d_1\nu_s}{385} + \frac{256c_{144}s_{44}d_2\nu_s}{175} + \frac{1024c_{144}s_{44}d_3\nu_s}{175} + \frac{256c_{456}s_{12}d_1\nu_s}{525}$$
$$+ \frac{256c_{456}s_{12}d_2\nu_s}{175} + \frac{2048c_{456}s_{12}d_3\nu_s}{525} + \frac{512c_{456}s_{44}d_1\nu_s}{385} + \frac{512c_{456}s_{44}d_2\nu_s}{175} + \frac{2048c_{456}s_{44}d_3\nu_s}{175} + \frac{1664s_{12}s_{44}d_1d_2}{1925}$$
$$+ \frac{768s_{12}s_{44}d_1d_3}{275} + \frac{256s_{12}s_{44}d_2d_3}{35} + \frac{128c_{12}s_{12}\nu\nu_s}{525} + \frac{256c_{12}s_{44}\nu\nu_s}{175} + \frac{256c_{44}s_{12}\nu\nu_s}{525} + \frac{512c_{44}s_{44}\nu\nu_s}{175}$$
$$+ \frac{128c_{144}s_{12}\nu\nu_s}{525} + \frac{256c_{144}s_{44}\nu\nu_s}{175} + \frac{256c_{456}s_{12}\nu\nu_s}{525} + \frac{512c_{456}s_{44}\nu\nu_s}{175} + \frac{1024s_{12}s_{44}d_1\nu}{1925} + \frac{256s_{12}s_{44}d_2\nu}{175}$$
$$+ \frac{768s_{12}s_{44}d_3\nu}{175} + \frac{832s_{12}d_1d_2\nu_s}{1925} + \frac{9088s_{12}d_1d_3\nu_s}{5775} + \frac{1152s_{12}d_2d_3\nu_s}{275} + \frac{384s_{44}d_1d_2\nu_s}{385} + \frac{157184s_{44}d_1d_3\nu_s}{35035}$$
$$+ \frac{18944s_{44}d_2d_3\nu_s}{1925} + \frac{2048s_{12}d_1\nu\nu_s}{5775} + \frac{384s_{12}d_2\nu\nu_s}{385} + \frac{17792s_{12}d_3\nu\nu_s}{5775} + \frac{3968s_{44}d_1\nu\nu_s}{3185} + \frac{5248s_{44}d_2\nu\nu_s}{1925} + \frac{4608s_{44}d_3\nu\nu_s}{385}. \quad \text{(C1)}$$

[1]G. Ghoshal, J. A. Turner, and R. L. Weaver, "Wigner distribution function of a transducer beam pattern within a multiple scattering formalism for heterogeneous solids," J. Acoust. Soc. Am. **122**, 2009–2021 (2007).
[2]G. Ghoshal and J. A. Turner, "Diffuse ultrasonic backscatter at normal incidence through a curved interface," J. Acoust. Soc. Am. **128**, 3449–3458 (2010).
[3]P. Hu, C. M. Kube, L. W. Koester, and J. A. Turner, "Mode-converted diffuse ultrasonic backscatter," J. Acoust. Soc. Am. **134**, 982–990 (2013).
[4]P. Hu and J. A. Turner, "Contribution of double scattering in diffuse ultrasonic backscatter measurements," J. Acoust. Soc. Am. **137**, 321–334 (2015).
[5]Y. Guo, R. B. Thompson, and F. J. Margetan, "Simultaneous measurement of grain size and shape from ultrasonic backscattering measurements made from a single surface," in *Review of Progress in Quantitative Nondestructive Evaluation*, Vol. 22, edited by D. O. Thompson and D. E. Chimenti (AIP, Melville, NY, 2003), pp. 1347–1354.
[6]O. I. Lobkis and S. I. Rokhlin, "Characterization of polycrystals with elongated duplex microstructure by inversion of ultrasonic backscattering data," Appl. Phys. Lett. **96**, 161905 (2010).
[7]O. I. Lobkis, L. Yang, J. Li, and S. I. Rokhlin, "Ultrasonic backscattering in polycrystals with elongated single phase and duplex microstructure," Ultrasonics **52**, 694–705 (2012).
[8]H. Du, C. Lonsdale, J. Oliver, B. M. Wilson, and J. A. Turner, "Evaluation of railroad wheel steel with lamellar duplex microstructures using diffused ultrasonic backscatter," J. Nondestruct. Eval. **32**, 331–340 (2013).
[9]H. Du, C. Lonsdale, J. Oliver, B. M. Wilson, and J. A. Turner, "Measurement of quench depth in railroad wheels by diffuse ultrasonic backscatter," J. Nondestruct. Eval. **33**, 104–110 (2014).
[10]H. Du and J. A. Turner, "Ultrasonic attenuation in pearlitic steel," Ultrasonics **54**, 882–887 (2014).
[11]P. Haldipur, F. J. Margetan, and R. B. Thompson, "Estimation of single-crystal elastic constants of polycrystalline materials from back-scattered grain noise," in *Review of Progress in Quantitative Nondestructive Evaluation*, Vol. 25, edited by D. O. Thompson and D. E. Chimenti (AIP, Melville, NY, 2006), pp. 1133–1140.
[12]J. Li, L. Yang, and S. I. Rokhlin, "Effect of texture and grain shape on ultrasonic backscattering in polycrystals," Ultrasonics **54**, 1789–1803 (2014).
[13]A. L. Pilchak, J. Li, and S. I. Rokhlin, "Quantitative comparison of micro-texture in near-alpha titanium measured by ultrasonic scattering and electron backscatter diffraction," Metall. Mater. Trans. A **45**, 4679–4697 (2014).
[14]B. Vrancken, R. Wauthle, J. P. Kruth, and J. Van Humbeeck, "Study of the influence of material properties on residual stress in selective laser

melting," in *Proceedings of the Twenty-Fourth Annual International Solid Freeform Fabrication Symposium* (August 2013), pp. 393–407.
[15]E. Todorov, R. Spencer, S. Gleeson, M. Jamshidinia, and S. M. Kelly, "Nondestructive evaluation (NDE) of complex metallic manufactured (AM) structures," in *America Makes: National Additive Manufacturing Innovation Institute (NAMII)*, AFRL Report, 2014, url: http://www.dtic.mil/dtic/tr/fulltext/u2/a612775.pdf (Last viewed August 3, 2015).
[16]M. F. Zaeh and G. Branner, "Investigations on residual stresses and deformations in selective laser melting," Prod. Eng. **4**, 35–45 (2010).
[17]J. A. Turner and G. Ghoshal, "Polycrystals under applied loads," Appl. Phys. Lett. **97**, 031907 (2010).
[18]C. M. Kube, H. Du, G. Ghoshal, and J. A. Turner, "Stress-dependent changes in the diffuse ultrasonic backscatter coefficient in steel: Experimental results," J. Acoust. Soc. Am. **132**, EL43–EL48 (2012).
[19]C. M. Kube, H. Du, G. Ghoshal, and J. A. Turner, "Measurement of thermally induced stresses in continuously welded rail through diffuse ultrasonic backscatter," in *Review of Progress in Quantitative Nondestructive Evaluation*, Vol. 31, edited by D. O. Thompson and D. E. Chimenti (AIP, Melville, NY, 2012), pp. 1673–1680.
[20]S. Hirsekorn, "The scattering of ultrasonic waves by polycrystals," J. Acoust. Soc. Am. **72**, 1021–1031 (1982).
[21]F. E. Stanke and G. S. Kino, "A unified theory for elastic wave propagation in polycrystalline materials," J. Acoust. Soc. Am. **75**, 665–681 (1984).
[22]R. L. Weaver, "Diffusivity of ultrasound in polycrystals," J. Mech. Phys. Solids **38**, 55–86 (1990).
[23]F. C. Karal and J. B. Keller, "Elastic, electromagnetic, and other waves in a random medium," J. Math. Phys. **5**, 537–547 (1964).
[24]S. Ahmed and R. B. Thompson, "Propagation of elastic waves in equiaxed stainless-steel polycrystals with aligned [001] axes," J. Acoust. Soc Am. **99**, 2086–2096 (1996).
[25]S. I. Rokhlin, J. Li, and G. Sha, "Far-field scattering model for wave propagation in random media," J. Acoust. Soc Am. **137**, 2655–2669 (2015).
[26]E. Kröner, "Statistical modeling," in *Modelling Small Deformations of Polycrystals*, edited by J. Gittus and J. Zarka (Elsevier Science Publishing Co., Inc., New York, 1986), pp. 229–291.
[27]E. Kröner, *Statistical Continuum Mechanics* (Springer-Verlag, Wien, 1972), 157 pp.
[28]S. Torquato, *Random Heterogeneous Materials: Microstructure and Macroscopic Properties* (Springer-Verlag, New York, 2005), 703 pp.
[29]P. R. Morris, "Averaging fourth-rank tensors with weight functions," J. Appl. Phys. **40**, 447–448 (1969).
[30]L. Yang and J. A. Turner, "Attenuation of ultrasonic waves in rolled metals," J. Acoust. Soc. Am. **116**, 3319–3327 (2004).
[31]C.-S. Man and W. Y. Lu, "Towards an acoustoelastic theory for measurement of residual stress," J. Elast. **17**, 159–182 (1987).
[32]C.-S. Man and R. Paroni, "On the separation of stress-induced and texture-induced birefringence in acoustoelasticity," J. Elast. **45**, 91–116 (1996).
[33]C.-S. Man, "Hartig's law and linear elasticity with initial stress," Inverse Probl. **14**, 313–319 (1998).
[34]C.-S. Man, "Effects of crystallographic texture on the acoustoelastic coefficients of polycrystals," Nondestruct. Test. Eval. **15**, 191–214 (1998).
[35]R. Paroni and C.-S. Man, "Constitutive equations of elastic polycrystalline materials," Arch. Rational Mech. Anal. **150**, 153–177 (1999).
[36]R. Paroni and C.-S. Man, "Two micromechanical models in acoustoelasticity: A comparative study," J. Elast. **59**, 145–173 (2000).
[37]M. Huang, H. Zhan, X. Lin, and H. Tang, "Constitutive relation of weakly anisotropic polycrystal with microstructure and initial stress," Acta. Mech. Sin. **23**, 183–198 (2007).
[38]D. S. Hughes and J. L. Kelly, "Second-order elastic deformation of solids," Phys. Rev. **92**, 1145–1149 (1953).
[39]R. A. Toupin and B. Bernstein, "Sound waves in deformed perfectly elastic materials. Acoustoelastic effect," J. Acoust. Soc. Am. **33**, 216–225 (1961).
[40]R. N. Thurston and K. Brugger, "Third-order elastic constants and the velocity of small amplitude waves in homogeneously stressed media," Phys. Rev. **133**, A1604–A1610 (1964).
[41]Y.-H. Pao, W. Sachse, and H. Fukuoka, "Acoustoelasticity and ultrasonic measurements of residual stress," in *Physical Acoustics*, Vol. XVII, edited by W. P. Mason and R. N. Thurston (Academic Press, New York, 1984).
[42]W. Voigt, "Theoretische studien über die elastizitätsverhältnisse der krystalle" ("Theoretical studies in the elastic behavior of crystals"), Abh. Kgl. Ges. Wiss. Göttingen. **34**, 3–51 (1887).
[43]J. P. Watt, D. F. Davies, and R. J. O'Connell, "The elastic properties of composite materials," Rev. Geophys. Space Phys. **14**, 541–563, doi:10.1029/RG014i004p00541 (1976).
[44]S. Hirsekorn, "Elastic properties of polycrystals: A review," Texture Microstruct. **12**, 1–14 (1990).
[45]C. M. Kube, "Acoustoelastic scattering and attenuation in polycrystalline materials," Ph.D. dissertation, University of Nebraska-Lincoln, Lincoln, NE, 2014.
[46]A. G. Every and A. K. McCurdy, "Second and higher-order elastic constants," in *Landolt-Börnstein Numerical Data and Functional Relationships in Science and Technology New Series Group III: Crystal and Solid State Physics*, Vol. 29, edited by O. Madelung and D. F. Nelson (Springer-Verlag, Berlin, 1992), 743 pp.
[47]G. C. Johnson, "Variations in the second- and third-order elastic constants in polycrystalline aggregates," J. Appl. Phys. **59**, 4057–4061 (1986).
[48]J. A. Turner and R. L. Weaver, "Radiative transfer and multiple scattering of diffuse ultrasound in polycrystalline media," J. Acoust. Soc. Am. **96**, 3675–3683 (1994).
[49]F. J. Margetan, P. Haldipur, and R. B. Thompson, "Looking for multiple scattering effects in backscattered ultrasonic noise from jet-engine nickel alloys," in *Review of Progress in Quantitative NDE*, Vol. 14, edited by D. O. Thompson and D. E. Chimenti (AIP, Melville, NY, 2005), pp. 2129–2136.
[50]S. Hirsekorn, "Theoretical description of ultrasonic propagation and scattering phenomena in polycrystalline structures aiming for simulations on nondestructive materials characterization and defect detection," in *Proceedings of the 11th ECNDT Conference*, Prague (2014), 10 pp.
[51]S. Hirsekorn, "The scattering of ultrasonic waves by multiphase polycrystals," J. Acoust. Soc. Am. **83**, 1231–1242 (1988).
[52]J. A. Turner and R. L. Weaver, "Radiative transfer of ultrasound," J. Acoust. Soc. Am. **96**, 3654–3674 (1994).
[53]J. A. Turner and R. L. Weaver, "Time dependence of multiply scattered diffuse ultrasound in polycrystalline media," J. Acoust. Soc. Am. **97**, 2639–2644 (1995).
[54]J. A. Turner and R. L. Weaver, "Ultrasonic radiative transfer in polycrystalline media: Effects of a fluid-solid interface," J. Acoust. Soc. Am. **98**, 2801–2808 (1995).
[55]T. P. Srinivasan and S. D. Nigam, "Invariant elastic constants for crystals," Phys. Stat. Solidi B **28**, K71–K73 (1968).
[56]K. Brugger, "Pure modes for elastic waves in crystals," J. Appl. Phys. **36**, 759–768 (1965).
[57]T. Y. Thomas, "On the stress-strain relations for cubic crystals," Proc. Natl. Acad. Sci. U.S.A. **55**, 235–239 (1966).
[58]G. R. Barsch, "Relation between third-order elastic constants of single crystals and polycrystals," J. Appl. Phys. **39**, 3780–3793 (1968).
[59]T. K. Ballabh, M. Paul, T. R. Middya, and A. N. Basu, "Theoretical multiple-scattering calculation of nonlinear elastic constants of disordered solids," Phys. Rev. B **45**, 2761–2771 (1992).
[60]N. Phan-Thien and R. A. Antonia, "Isotropic Cartesian tensors of arbitrary even orders and velocity gradient correlation functions," Phys. Fluids **6**, 3818–3822 (1994).
[61]G. Wagnière, "The evaluation of three-dimensional rotational averages," J. Chem. Phys. **76**, 473–480 (1982).